8-9-2012

# Green Tea Extract Protects Against Fibrogenesis Associated with Nonalcoholic Fatty Liver Disease in Diet-Induced Obese Rats

Allyson M. Bower
*University of Connecticut - Storrs*, allyson.bower@gmail.com

# Green Tea Extract Protects Against Fibrogenesis Associated with Nonalcoholic Fatty Liver Disease in Diet-Induced Obese Rats

Allyson M. Bower, B.S.

University of Connecticut

A Thesis Submitted in
Partial Fulfillment of the
Requirements for the Degree of
Master of Science at the
University of Connecticut

2012

# Approval Page

Master of Science Thesis

Green Tea Extract Protects Against Fibrogenesis Associated with Nonalcoholic Fatty Liver Disease in Diet-Induced Obese Rats

Presented by

Allyson M. Bower, B.S.

Major Advisor _____
Richard S. Bruno, Ph.D., R.D

Associate Advisor _____
Ji-young Lee, Ph.D.

Associate Advisor _____
Hedley C. Freake, Ph.D.

University of Connecticut

2012

# Acknowledgements

First and foremost I would like to thank Dr. Richard Bruno for the valuable guidance, insight and enthusiasm he provided me throughout the course of my time here at UConn and for his ability to ask all of the right questions. I am a better scientist because of it. I would also like to thank him for accepting me into his lab as an undergraduate and supporting my interest in molecular biology.

I would also like to thank the members of the Bruno Lab, past and present. Specifically, I would like to thank Chris Masterjohn for his valuable scientific input in the lab and for the valuable editorial input he provided throughout my writing process. I would also like to thank Yi Guo, Eunice Mah and Ruisong Pei for their eternal optimism, making the lab and office both wonderful places to work. I would also like to thank Min-Yu Chung and Hea-Jin Park. Without their hard work, this project would not have existed. I would also like to express my gratitude to the department of Nutritional Sciences for providing me with an environment where I could discover and expand upon my passion for nutrition.

Lastly, I would like to thank my family for their endless support of my education and scientific endeavors and for providing me with a comforting home environment where I could work and study. I would also like to thank my boyfriend Billy Jenkins for staying by my side throughout my education and always being there for me when I needed him.

# Table of Contents

# List of Figures

# List of Tables

# List of Abbreviations

| | |
|---|---|
| 4-hydroxynonenol | 4-HNE |
| advanced glycation end products | AGE |
| alanine aminotransferase | ALT |
| aspartate aminotransferase | AST |
| CCAAT/enhancer-binding protein-β | C/EPBβ |
| carbon tetrachloride | CCl4 |
| cytochrome$P_{450}$2E1 | CYP2E1 |
| cytochrome$P_{450}$2E1 | CYP4A |
| epicatechin | EC |
| extracellular matrix | ECM |
| epicatechin gallate | ECG |
| epigallocatechin | EGC |
| epigallocatechin gallate | EGCG |
| glutamate cysteine ligase | GCL |
| catalytic subunit of glutatmate cysteine ligase | GCLc |
| glutathione | GSH |
| green tea extract | GTE |
| homeostatic model of insulin resistance | HOMA-IR |
| horseradish peroxidase | HRP |
| hepatic stellate cells | HSC |
| inhibitor of nuclear factor-κB kinase subunit-β | IKK-β |
| insulin receptor substrate-1 | IRS-1 |
| Kruppel-like factor 6 | KLF6 |
| monocyte chemoattractant protein-1 | MCP-1 |
| malondialdehyde | MDA |
| nicotinamide adenine dinucleotide phosphate | NADPH |
| nonalcoholic fatty liver disease | NAFLD |
| nonalcoholic steatohepatitis | NASH |
| nuclear factor κB | NFκB |
| platelet derived growth factor | PDGF |
| β-type platelet derived growth factor receptor | PDGF-Rβ |
| reactive oxygen species | ROS |
| sterol regulatory element binding protein-1c | SREBP-1c |
| thiobarbituric acid reactive substances | TBARS |
| transforming growth factor β1 | TGFβ1 |
| total hepatic glutathione | tGSH |
| tumor necrosis factor receptor-1 | TNF-R1 |
| tumor necrosis factor-α | TNF-α |

# Abstract

Nonalcoholic fatty liver disease (NAFLD) is a constellation of diseases ranging from hepatic steatosis to fibrosis, cirrhosis and potentially liver-related mortality. Estimates indicate that NAFLD affects 80-90% of obese individuals. No validated treatments exist for NAFLD beyond weight loss and lifestyle modifications, but these approaches have poor long-term adherence. This indicates a need to validate effective therapies that prevent the progression of NAFLD. Oxidative stress potentiates fibrosis by activating hepatic stellate cells (HSCs), which in turn deposit hepatic collagen. Consistent with earlier findings suggesting that green tea extract (GTE) mitigates hepatic steatosis and oxidative stress, we hypothesized that GTE would attenuate the fibrosis associated with NAFLD. Wistar rats (n = 63) were fed a low-fat diet (LFD) containing no GTE or high-fat diet (HFD) containing GTE at 0, 1 or 2% GTE for 8 wk. Fibrosis was visualized by Gomori's trichrome stain and corroborated by measuring the collagen marker hydroxyproline (HYP). α-Smooth muscle actin (α-SMA), an indicator of HSC activation, and nuclear KLF6 protein were measured by western blot. Rats in the HFD group had histologic evidence of fibrosis and greater HYP than rats fed the LFD. Rats fed GTE at either level had little or no visible evidence of fibrosis and HYP levels were normalized to the extent of LFD controls. Rats fed the HFD had greater hepatic α-SMA expression compared to the LFD group whereas α-SMA in the HFD + 2% GTE group was not different from the LFD group. The HFD increased nuclear KLF6 accumulation relative to the LFD group, but was unaffected by GTE. α-SMA and HYP were correlated with serum AST and inversely related to hepatic total glutathione, suggesting that liver injury mediated by oxidative stress contributes to fibrosis. Collectively, these data indicate that

GTE protects against HFD-induced fibrosis by preventing HSCs activation and collagen deposition through a mechanism independent of the transcription factor KLF6.

# Chapter 1: Introduction

Nonalcoholic fatty liver disease (NAFLD) is a constellation of diseases that progress from relatively benign steatosis to nonalcoholic steatohepatitis (NASH), fibrosis, cirrhosis, hepatocellular carcinoma and eventually liver-related mortality [1]. NAFLD is estimated to affect 10-30% of Americans [2] and is closely associated with obesity with estimates indicating that 80-90% of obese individuals are afflicted with this disorder [3]. It is estimated that one-third of individuals with steatosis will develop NASH, and in turn, 33% of those individuals will develop fibrosis and 15% will develop cirrhosis [4]. There is no validated treatment for NAFLD beyond weight loss and co-morbidity management and lifestyle modification [5], but these interventions have poor long term adherence [6]. This necessitates the identification of both a simple and effective therapy aimed at preventing the progression of this disease.

The development of NASH is most frequently described by the "two-hit" mechanism [7]. Liver steatosis is the "first hit" and encompasses metabolic disruptions associated with obesity. These disruptions, such as insulin or leptin resistance, cause excessive accumulation of fat in the liver [7]. Hepatic steatosis increases the vulnerability of the liver to a "second hit" in the form of lipid peroxidation initiated by oxidative stress, resulting from a number of factors including mitochondrial dysfunction, microsomal oxidation of fatty acids, and inflammatory cell infiltration [5].

Oxidative stress and inflammation associated with NASH induce hepatic stellate cell (HSC) activation. Activated HSCs adopt a myofibroblastic phenotype characterized by expression of α-smooth muscle actin (α-SMA) [1, 8] and begin producing extracellular matrix (ECM) proteins [1]. Once activated, HSCs also begin expressing

inflammatory cytokines and fibrogenic cytokines. This signaling cascade exacerbates inflammation and oxidative stress and results in fibrosis [1].

A transcription factor Kruppel-like factor 6 (KLF6) has been identified in carbon tetrachloride ($CCl_4$) and methionine and choline deficiency models of hepatic fibrosis but not in simple steatosis [9]. mRNA levels of this transcription factor are modulated by oxidative stress [9] and KLF6 promotes the expression of several important pro-fibrogenic proteins such as procollagen(α1)I [10, 11]. The mechanism by which KLF6 is activated and translocated into the nucleus has not yet been elucidated. However, during hepatic fibrosis KLF6 is localized in the nuclear and perinuclear area suggesting that nuclear translocation occurs during this process [11].

Because oxidative stress and inflammation promote the progression of steatosis to fibrosis, it is logical that dietary approaches that counter oxidative stress and inflammation may prevent fibrogenesis. The bioactive components of green tea (*Camellia sinensis*) have hypolipidemic [12], anti-inflammatory [13] and antioxidant [14] properties. Furthermore, epidemiological studies suggest that there is in an inverse association between green tea consumption and all-cause mortality and mortality due to cardiovascular disease [15] and that consuming >10 cups/d may protect against liver injury [16].

Previous work in our lab has defined a diet-induced obese model of NASH in rats, the consequences of which are mitigated by green tea extract (GTE). Our group has determined that rats consuming 60% of energy from fat for 8 wk have significant increases in hepatic levels of the inflammatory cytokines tumor necrosis factor-α (TNF-α) and monocyte chemoattractant protein-1 (MCP-1) as well as increased nuclear binding

of the pro-inflammatory transcriptional factor nuclear factor-κB (NFκB). Additionally, hepatic glutathione (GSH) in these animals was depleted, indicating increased oxidative stress. When rats were provided with the GTE equivalent to 7-14 cups/day in humans in addition to the high-fat diet (HFD), they had significantly lower concentrations of the previously mentioned biomarkers for inflammation and maintained GSH status [13]. Since previous reports indicate that rats consuming a diet of 30% energy from fat for 12 weeks develop NASH and fibrosis [17, 18], it is hypothesized that this model of NASH will also develop fibrosis.

The central hypothesis of this thesis is that GTE will protect against fibrosis in a HFD-induced model of NAFLD. It is hypothesized that this effect will be accompanied by decreased HSC activation, since HSCs are activated via inflammatory signaling and oxidative stress and GTE has antioxidant and anti-inflammatory properties. It is also hypothesized that GTE will decrease KLF6 nuclear protein because of its antioxidant properties. To test these hypotheses, the following objectives were completed.

- **Objective 1**: Define to what extent GTE prevents fibrosis associated with high-fat feeding. To visualize fibrosis, liver tissue was stained with Gomori's trichrome, which differentiates connective tissue from cytoplasm and nuclei. To quantify hepatic collagen accumulation, hepatic hydroxyproline concentration was measured as an indirect indicator of hepatic collagen deposition.
- **Objective 2**: Define to what extent GTE prevents HSC activation associated with high-fat feeding. To test this hypothesis, hepatic protein expression of α-

SMA, a protein expressed by HSCs, was measured by western blot and subsequent densitometry.

- **Objective 3**: Define to what extent GTE prevents nuclear protein accumulation of KLF6. To test this hypothesis, nuclear extracts were prepared from liver homogenate and KLF6 protein accumulation was analyzed via western blot and subsequent densitometry.

When studies from this thesis are completed, it is expected that rats fed a diet containing 60% energy from fat for 8 wk will develop hepatic fibrosis. It is also expected that feeding rats the GTE equivalent to 7-14 cups of green tea per day in humans in addition to the HFD will mitigate fibrosis and hepatic collagen deposition and that this will be accompanied by decreased HSC activation. It is expected that the findings in this thesis will support the investigation of increasing green tea consumption in humans as a strategy for preventing fibrosis associated with NAFLD.

# Chapter 2: Review of Literature

## *2.1 Introduction*

Steatosis potentiates the development of nonalcoholic steatohepatitis (NASH) and fibrosis. These conditions are referred to as nonalcoholic fatty liver disease (NAFLD) and increase liver-related morbidity and mortality. Oxidative stress plays an important role in disease progression from steatosis to fibrosis. Thus, therapies aimed at reducing oxidative stress in the liver may play a role in reducing progression of NAFLD. This literature review will introduce the prevalence of NAFLD and its diagnosis, then discuss the etiology of steatosis, NASH and fibrosis in the context of obesity. Next, various diet-induced animal studies of NAFLD will be discussed to support diet-induced obesity as a model of fibrosis. Lastly, since this thesis project is examining GTE as a novel strategy to regulate fibrosis, a discussion of the hepatoprotective properties of green tea will be provided.

## *2.2 Epidemiology of NAFLD*

At present, it is estimated that between 10-30% of Americans have some stage of NAFLD [2]. NAFLD begins with fat accumulation in the liver otherwise known as steatosis [7]. It is estimated that one-third of those with simple steatosis will develop NASH. Of those who develop NASH, 33% will develop fibrosis and 15% will develop cirrhosis [4]. Several independent predictors for disease progression into fibrosis have been identified, such as elevated fasting blood glucose, decreased insulin sensitivity [19] and elevated body mass index (BMI) [20]. Data from NHANES III indicates that individuals with NAFLD have greater liver-related mortality than individuals who do not have NAFLD [21]. Among individuals with NAFLD, liver disease was the third leading

cause of death [21]. For comparison, liver disease was the 11th leading cause of death among individuals without NAFLD [21]. Taken together, these data suggest that NAFLD increases liver-related morbidity and mortality.

One of the challenges in identifying the rates of NAFLD in the population is the difficulty in diagnosing the condition. The gold standard for diagnosing NAFLD is liver biopsy, however this procedure is quite invasive [1]. Ultrasonography can also be used. Ultrasonography has a sensitivity of 89% and a specificity of 93% in detecting steatosis and a sensitivity of 77% and a specificity 89% in detecting the stage of fibrosis [22]. The simplest technique for identifying potential cases of NAFLD is blood testing for the liver transaminases aspartate aminotransferase (AST) and alanine aminotransferase (ALT), but NAFLD can be present in as many as 50% of individuals that do not have elevated liver enzymes [3]. The sensitivity of ALT alone in detecting NAFLD is 45% [23]. The positive predictive value for using both AST and ALT to diagnose NAFLD is 90% while it is 34% for diagnosing NASH [23]. ALT is an enzyme that resides primarily in hepatocyte cytoplasm, while AST resides primarily in hepatocyte mitochondria [24]. For this reason ALT is often considered a more reliable biomarker for hepatocyte injury than AST. However, research on the use of AST alone as diagnostic criteria for extensive liver injury suggests that it may be more useful than ALT in determining the degree of necroinflammation [25] and liver damage [26]. Brunt et al [25] report that mean AST levels were higher in NAFLD patients with severe histological scoring of necroinflammation compared to the AST levels measured in those with mild or moderate scoring ($P < 0.002$, $P < 0.05$) while there were no differences between ALT values and disease severity ($P > 0.05$). Additionally, multivariate stepwise regression analyses of

various predictors of histological damage to the liver indicated AST values were the most important predictive variable of histological activity (r = 0.62) in patients with the hepatic C virus. [26]. One hypothesis for this suggests that as degree of liver injury increases, the degree of mitochondrial damage increases which thus increases blood levels of AST [26].

The provided specificities and positive predictive values indicate that serum aminotransferases and ultrasonography underestimate the prevalence of NAFLD. Because simple steatosis can develop into fibrosis [1], preventative measures should be taken in individuals at risk for NAFLD. At present, there is no validated treatment of NAFLD besides weight loss and lifestyle intervention, however these treatments have low compliance [6]. This necessitates the identification of simple dietary interventions that can prevent the progression of NAFLD.

### *2.3 Development of Steatosis*

Steatosis, or fat accumulation in the liver, is the initial stage of NAFLD and is often referred to as the "first hit" leading to NASH and fibrosis [7]. Histologically, grade one of steatosis is diagnosed when <33% of hepatocytes are affected, the second grade is diagnosed when between 33-66% of hepatocytes are affected and the third grade is diagnosed when >66% of hepatocytes are affected [5]. Thus, interventions aimed at preventing steatosis may be successful in limiting the progression of NAFLD.

Obesity plays a significant role in developing steatosis since it potentiates the development of insulin resistance and type II diabetes [27]. In fact, the prevalence of NAFLD is between 80–90% in obese adults and between 30–50% in patients with type II diabetes [3]. The mechanisms behind the development of steatosis from obesity and diabetes will be explained in the following paragraphs.

*2.3.1 Obesity*

Obesity leads to macrophage infiltration of adipose tissue, which results in increased inflammatory signaling [28]. Microarray analysis performed on white adipose tissue from *ob/ob* mice indicated that 59% of all of the genes that were upregulated more than 2-fold over the lean control could be classified as inflammation-related genes. The remaining genes were related to other diverse molecular pathways such as fat storage, cholesterol metabolism or cell division. Histological staining of the adipose tissue indicated that tissue from *ob/ob* mice had significant macrophage infiltration compared to the lean control. The adipose tissue from *ob/ob* mice was also separated into its adipocyte and stromal-vascular fractions. Analysis of mRNA in these tissue fractions indicated that the stromal-vascular fraction expressed significantly greater mRNA for tumor necrosis factor-α (TNF-α) [29]. These results suggest that macrophage infiltration of adipocytes in obese mice leads to increased expression of the pro-inflammatory cytokine TNF-α. This hypothesis is supported by observations in humans. Explanted adipose tissue from obese post-menopausal women (BMI > 25) produced significantly greater TNF-α mRNA and protein compared to biopsied tissue from lean controls (BMI < 25). There was also a significant positive correlation ($r = 0.82$) between TNF-α mRNA production by adipose tissue and plasma insulin levels indicating that greater TNF-α expression from adipose tissue correlates to reduced insulin sensitivity [30]. Thus, obesity increases systemic inflammation and contributes to insulin resistance which can lead to hepatic steatosis.

*2.3.2 Insulin Resistance*

The pro-inflammatory cytokine TNF-α is increased in obese individuals and correlates with insulin sensitivity [30]. TNF-α interferes with the signaling cascade

downstream of the insulin receptor resulting in insulin resistance [30]. When insulin binds to the insulin receptor, the insulin receptor phosphorylates insulin receptor substrate-1 (IRS-1) on its tyrosine residue. In adipose and muscle tissue, however, IRS-1 is phosphorylated on a serine residue in response to stressors, including TNF-α. IRS-1 phosphorylated at this location does not respond to the insulin receptor [28]. Treatment of adipocytes with 2.5 ng/ml of TNF-α resulted in decreased phosphorylation of IRS-1 on the tyrosine residue [31]. This interruption in the signaling cascade has direct effects on the levels of glucose in the blood as the glucose transporter type 4 is no longer translocated to the cell surface [31]. Excessive blood glucose that results from decreased insulin sensitivity leads to a greater release of insulin by pancreatic β-cells and eventually leads to an excess of blood insulin, termed hyperinsulinemia [32].

*2.3.3 Steatosis*

Elevated blood insulin contributes to steatosis by increasing *de novo* lipogenesis. When isolated hepatocytes from rats treated with streptozotocin to induce diabetes were treated with insulin *in vitro*, the result was an in increase in sterol regulatory element binding protein-1c (SREBP-1c) mRNA levels and nuclear protein levels of this transcription factor [33]. Additionally, hyperinsulinemic *ob/ob* mice expressed greater hepatic SREBP-1c mRNA in addition to mRNA of its downstream target genes, fatty acid synthase and acetyl-CoA carboxylase [34]. This presents a paradox in that during insulin resistance, the liver is still selectively responsive to insulin.

The liver displays selective insulin sensitivity due to its differential response to TNF-α. Insulin resistant adipose tissue and muscle tissue taken from obese Zucker rats had reduced insulin receptor tyrosine phosphorylation of IRS-1. However, no significant

changes were observed in insulin-stimulated tyrosine phosphorylation of IRS-1 in hepatic tissue from these animals [35]. This suggests that TNF-α does not mediate hepatic insulin resistance in the same way as it does in muscle or adipose tissue. During selective hepatic insulin resistance, insulin fails to suppress gluconeogenic enzymes such as phosphoenolpyruvate carboxykinase or glucose-6-phosphatase, yet it increases transcription and nuclear translocation of SREBP-1c which upregulates genes associated with *de novo* lipogenesis [36]. The reason for this is bifurcation of the insulin signaling pathway downstream of the kinase Akt [37]. Inhibition of Akt augments gluconeogenic gene expression and reduces SREBP-1c upregulation of lipogenic gene expression. In contrast, inhibition of a kinase downstream of Akt, mammalian target of rapamycin complex 1, results in augmented gluconeogenic genes and increased SREBP-1c upregulation of lipogenic genes, the characteristic insulin response seen in type 2 diabetes [37]. Thus, hyperinsulinemia and selective hepatic insulin resistance contributes to enhanced lipogenesis.

Besides increasing *de novo* lipogenesis, SREBP-1c contributes to steatosis by decreasing β-oxidation. SREBP-1c upregulates acetyl-CoA carboxylase. Acetyl-CoA carboxylase adds a carboxyl group to acetyl-CoA, resulting in the formation of malonyl-CoA. Malonyl-CoA is an inhibitor of the enzyme carnitine palmitoyl transferase-1. Carnitine palmitoyl transferase-1shuttles fatty acids into the mitochondria for β-oxidation [38]. Thus, upregulation of acetyl-CoA carboxylase by SREBP-1c during insulin resistance contributes to hepatic steatosis by inhibiting β-oxidation of fatty acids.

Insulin resistance also leads to steatosis by increasing circulating free fatty acids . Insulin suppresses the activity of the enzyme hormone sensitive lipase in insulin sensitive

individuals, however insulin resistance increases its activity. Since hormone sensitive lipase is responsible for lipolysis in adipose tissue, insulin resistant adipose tissue releases excess free fatty acids into the blood [39]. Insulin resistant hepatocytes then uptake these free fatty acids [5], contributing to steatosis.

### *2.4 Development of NASH*

Histologically, NASH is diagnosed when steatosis involves more than 66% of hepatic lobules, ballooning hepatocytes are observed indicating hepatocellular damage, and there is mild infiltration of the hepatic lobules by polymorphonuclear and mononuclear cells, indicating the presence of inflammation [5]. Fat accumulation in the liver does not always lead to necroinflammation and progression of NASH or fibrosis. This prompted the suggestion of oxidative stress as the "second hit" involved in the pathogenesis of NAFLD [7]. Oxidative stress initiates lipid peroxidation in the lipid-laden steatotic liver, leading to cellular damage and inflammation [27]. Therapies aimed at mitigating oxidative stress may therefore be successful in limiting the progression of steatosis to fibrosis. The sources and consequences of oxidative stress are introduced below.

#### *2.4.1 Sources of Oxidative Stress*

The mitochondria are one source of oxidative stress in the liver during NAFLD. Hepatic fatty acids are metabolized via mitochondrial β-oxidation which, under conditions associated with NAFLD, generates greater reactive oxygen species (ROS). Mitochondria isolated from *ob/ob* mice produced superoxide anions at a greater rate than mitochondria isolated from control mice, indicating a role for obesity in hepatic mitochondrial dysfunction [40]. This process may be initiated by the pro-inflammatory

cytokine TNF-α, since cells cultured with TNF-α have been shown to inhibit mitochondrial electron transport chain activity [41]. As a result of continued metabolism under these conditions, there is over-reduction of the electron transport chain which leads to leakage of the superoxide anion [42]. Thus, obesity and inflammation result in greater hepatic oxidative stress and contribute to the second hit of NASH.

Other sources of hepatic oxidative stress in NAFLD are cytochrome $P_{450}$ enzymes, more specifically, cytochrome $P_{450}$2E1 (CYP2E1) and cytochrome $P_{450}$4A (CYP4A). These cytochrome $P_{450}$ enzymes are located in the endoplasmic reticulum of hepatocytes and the primary function of these cytochrome $P_{450}$ enzymes is to detoxify lipophilic compounds by hydroxylation [43]. CYP2E1 is upregulated during hepatic insulin resistance [44] and free fatty acid accumulation in the liver upregulates CYP4A [45]. Cytochrome $P_{450}$ enzymes require electrons to be donated by the enzyme nicotinamide adenine dinucleotide phosphate (NADPH)-cytochrome $P_{450}$ reductase to complete hydroxylation, but the activities of these 2 enzymes are poorly coupled, resulting in the generation of superoxide [43]. Peroxisomal β-oxidation of excess fatty acids also contributes to hepatic oxidative stress. In the initial step of peroxisomal β-oxidation, $H_2O_2$ is formed by the action of acyl-CoA oxidase, which donates electrons directly to molecular oxygen [38]. Free fatty acids induce transcription of acyl-coA oxidase [46] and increase peroxisomal β-oxidation and production of $H_2O_2$ [38]. Thus, induction of CYP2E1 and CYP4A in addition to peroxisomal β-oxidation in the steatotic liver generates oxidative stress [47].

Another source of oxidative stress in the liver is apoptotic hepatocytes. Biopsies from individuals with NASH showed 2.7-fold increase in histological staining for the

death receptor tumor necrosis factor receptor-1 (TNF-R1) compared to biopsies from healthy individuals, and staining intensity for TNF-R1 correlated to disease severity [48]. TNF-α binding to TNF-R1 initiates apoptosis by inducing DNA fragmentation [49] and the release of ROS from the mitochondria [40]. Furthermore, apoptotic hepatocytes release pro-inflammatory mediators, which attracts Kupffer cells and neutrophils [1]. In an inflammatory environment, these cells of the immune system produce superoxide anions through NADPH-oxidase in a phenomenon referred to as "oxidative burst" [50]. Thus hepatocyte apoptosis leads to direct release of ROS into the environment from the mitochondria during apoptosis and initiates immune cell infiltration of the liver which also contributes to the release of ROS in the pathogenesis of NASH.

*2.4.2 Consequences of Oxidative Stress*

Oxidative stress from the above sources leads to lipid peroxidation, which further contributes to the hepatic damage observed in NASH [27]. Lipid peroxidation is the process by which lipids are converted to lipid hydroperoxides by the oxidation of a polyunsaturated fatty acid by oxidants such as superoxide or hydroxyl radicals [51]. The formation of lipid hydroperoxides potentiates the formation of additional lipid peroxidation through the formation of the lipid radical [51]. Lipid peroxidation can directly damage cell membranes which results in loss of membrane fluidity and eventually leading to necrosis [27]. Additionally, lipid peroxidation of the phospholipid-rich mitochondria can further lead to mitochondrial dysfunction and release of ROS into the environment [38]. Lipid hydroperoxides are also detrimental in that they auto-oxidize to form the cytotoxic molecules 4-hydroxynonenal (4-HNE) and malondialdehyde (MDA) [52] which are harmful in that they bind to mitochondrial DNA [53], nuclear

DNA [54] and proteins [55], which may initiate the immune response or inactivate important enzymes [27]. Because the steatotic liver contains an excess of lipids, it is especially prone to the harmful effects of the lipid peroxidation [7].

Lipid peroxidation also contributes directly to steatosis. The lipid peroxidation end products thiobarbituric acid reactive substrates (TBARS) are associated with increased post-ER presecretory proteolysis of ApoB100 [56]. Incubation of hepatocytes with ω-6 and ω-3 polyunsaturated fatty acids increased ApoB100 degradation via intracellular induction of TBARSs and this effect was not observed when the antioxidant vitamin E was added to the media [56]. Thus, oxidative stress limits very low density lipoprotein secretion by the liver and increases fat accumulation in the liver.

### *2.5 Development of Fibrosis*

#### *2.5.1 Overview*

Taken together, all of the causes and consequences of steatosis and NASH lead to hepatic damage and initiate the process of fibrogenesis [1]. Fibrogenesis begins with the activation of HSCs [27]. In the healthy liver, HSCs constitute less than 10% of total resident cell population and reside in the space of Disse between the sinusoidal endothelium and the hepatocyte chords within the liver lobule (**Figure 2.1A**) [57]. Once activated, HSCs increase in number and adopt a myofibroblastic phenotype and express the structural protein α-smooth muscle actin (α-SMA). With this new phenotype, HSCs begin to produce pro-inflammatory and pro-fibrogenic cytokines. Activated HSCs are also the primary source of ECM components deposited during fibrosis [58], and by reducing HSC activation, it may be possible to prevent fibrosis.

Fibrosis is defined as the remodeling of the ECM to contain primarily type I collagen [1]. In the healthy liver, the ECM provides a low-density barrier between the sinusoids and the cords of hepatocytes (**Figure 2.1A**). The low density of this barrier, in addition to the porous arrangement of endothelial cells, allows free exchange between liver cells and blood flow [59]. Changes in the ECM brought on by fibrogenesis in the perisinusoidal space interrupt blood flow to the hepatocytes [60]. Under fibrogenic conditions, the quantity of ECM components can increase 3-5 fold, with a shift towards a composition of primarily the fibrillar collagens type I and III and away from lower-density collagen type IV [57]. This process is referred to as sinusoidal capillarization and results in further hepatocyte dysfunction and portal hypertension due to decreased blood flow to the hepatocytes. Thus, fibrosis contributes the advanced diseases cirrhosis and hepatocellular carcinoma [60]. The etiology of the liver injury dictates where fibrogenesis begins, and in the case of NAFLD, fibrosis begins in the pericellular and perisinusoidal space in zone III of the liver lobule [25] (**Figure 2.1B**).

*2.5.2 Causes of Fibrosis*

Oxidative stress activates HSCs, thereby linking the second hit of NASH to fibrogenesis. When quiescent HSCs were incubated with ROS-generating CYP2E1-overexpressing HepG2 cells, they expressed more α-SMA compared to HSCs incubated with control HepG2 cells. This suggests greater HSC activation is a result of an environment containing greater ROS. HSCs also expressed more intracellular and secreted collagen type I protein than HSCs incubated with conventional HepG2 cells. This effect was abrogated by the addition of vitamin E or catalase to the co-culture. [61]. Additionally, human HSCs incubated directly with the lipid peroxidation product 4-HNE

produced more procollagen(α1)I mRNA and type I collagen protein compared to control culture [62].

Fibrosis is also associated with the second hit of NASH through greater Kupffer cell activity. In NASH, Kupffer cells release the cytokines TNF-α and transforming growth factor β1 (TGFβ1). TNF-α promotes the inflammatory response and activates HSCs [1]. Activation of inhibitor of nuclear factor-κB kinase subunit-β (IKK-β) by TNF-α induces nuclear translocation of the transcription factor nuclear factor-κB (NFκB). NFκB nuclear activity upregulates monocyte chemoattractant protein-1 (MCP-1) [63] and TNF-α expression [64]. Thus, TNF-α activation of NFκB further promotes insulin resistance and the inflammatory response. Additionally, it has been shown that incubation of TNF-α with HSCs increases the transcription of TGFβ1 receptor type I [65] and in this way promotes the pro-fibrogenic response in addition to its pro-inflammatory effect.

TGFβ1 is responsible for the pro-fibrogenic response in HSCs by promoting the transcription of various ECM proteins, including the most prevalent collagen in fibrosis, collagen type I. TGFβ1 increases expression of the procollagen(α1)I gene in HSC by promoting the formation of $H_2O_2$. Accumulation of intracellular $H_2O_2$ stimulates expression of the p35 isoform of CCAAT/enhancer-binding protein-β (C/EBPβ) and promotes binding of this factor to a TGFβ1 responsive element located the procollagen(α1)I gene promoter [66]. To promote further fiber accumulation, TGFβ1 also induces the expression of the collagenase inhibitor, tissue inhibitor of matrix metalloproteinases-1 [67].

Additionally, TGFβ1 promotes fibrosis by increasing HSC proliferation. The principle mitogen for HSC is platelet-derived growth factor (PDGF) [68], which is

expressed by activated Kupffer cells in damaged liver [69]. TGFβ1 receptor binding increases expression of β-type platelet derived growth factor receptor (PDGF-Rβ) [67] and in this way facilitates HSC proliferation and promotes fibrogenesis. NFκB has also been identified as a promoter of PDGF-Rβ expression [70]. This suggests a potential role for TNF-α, or other upstream activators of NFκB, in HSC proliferation.

TGFβ1 is also responsible for propagating the pro-fibrogenic response by inducing further TGFβ1 production. Quiescent HSCs express low levels of TGFβ1 receptors, while activated HSCs express more mRNA for TGFβ1 receptor type I and TGFβ1 receptor type II. This has been shown to be a direct result of TGFβ1 binding, which indicates that TGFβ1 propagates the pro-fibrogenic response in an autocrine manner [71]. Additionally, TGFβ1 signaling promotes the expression of intracellular α-SMA via the Smad3 signaling pathway [72], indicating its involvement in changing the HSC phenotype.

Direct consequences of obesity such as type II diabetes also play a role in HSC activation. HSCs express receptors for advanced glycation end products (AGE) which are elevated in diabetic individuals [73] and AGE receptor binding promotes HSC activation [74]. Also elevated in diabetic individuals is angiotensin type II. Angiotensin type I receptors bind to angiontensin type II and promote vasoconstriction in peripheral tissue. Angiotensin type I receptors are present on both quiescent and activated HSCs and angiotensin type I receptor binding by angiotensin type II stimulates ECM secretion, HSC proliferation, release of inflammatory cytokines, release of growth factors and inhibitors of collagen degradation [74].

Obese individuals also often develop leptin resistance and as a result have elevated blood leptin. The leptin deficient *ob/ob* model of NAFLD does not exhibit a fibrogenic phenotype, while repletion of leptin in this system allows for the disease progression into fibrosis [75]. This indicates that leptin is essential to the hepatic fibrogenic response. Leptin plays an role in fibrosis by modulating levels of free TGFβ1 and it has been hypothesized that this may be due to increased transcription of urokinase-like plasminogen activator, which is responsible for activating plasmin which frees TGFβ1 from its latency-associated peptide [75]. Leptin binding to its receptors also signals direct upregulation of TGFβ1 protein itself through the STAT3 and STAT5 signaling pathway [76]. Leptin has also been shown to increase HSC expression of PDGF-Rβ [77] and thus increases HSC proliferation.

The ECM also plays a role in activation of HSCs. Quiescent HSCs cultured on matrigel, a surface containing basement membrane components, maintain their quiescent phenotype. When cultured on polystyrene, a type I collagen coated dish or a type IV collagen coated dish, HSCs exhibited their activated phenotype [78, 79]. The environment also dictates how HSCs respond to external stimuli. When TGFβ1 was added to HSCs cultured on type I collagen-coated culture dishes, collagen synthesis of the cells grown on type I collagen-coated dishes was stimulated. Conversely, there was no response to TGFβ1 in terms of collagen synthesis by the HSCs grown on a dish coated in type IV collagen. Thus, the reaction of HSCs to cytokines is also modulated by ECM [80].

A transcription factor that upregulates collagen during fibrosis is KLF6. In 1998, Vlad Ratziu and his colleagues [10] isolated HSCs from rats administered $CCl_4$ and

identified the transcript for a molecule containing a zinc-finger motif, suggesting the presence of a novel transcription factor associated with hepatic injury. They further defined this molecule as the transcription factor Zf9 [10] which would later be named KLF6 because of its structural similarity to other proteins in the Kruppel-like factor family of transcription factors [81]. KLF6 is localized in the nuclear and perinuclear space in HSCs isolated from rats injected with $CCl_4$ to induce liver injury, and *in vivo* expression and biosynthesis of this protein is increased in response to liver injury with $CCl_4$ [11].

These results prompted further research into identifying the target genes associated with this transcription factor. Ratziu et al [10, 11] have shown that KLF6 upregulates the transcription of procollagen(α1)I as well as the pro-fibrogenic cytokine TGFβ1 and its receptors type I and II. Additionally, KLF6 increases transcription of urokinase-like plasminogen activator, a molecule that cleaves plasminogen to plasmin, whose role in fibrosis is to free TGFβ1 from its latency-associated peptide allowing it to bind to its receptors [82].

Upregulation of KLF6 has been evidenced in $CCl_4$-induced liver injury [11] and in the methionine choline deficient diet models of steatohepatitis [9]. However, KLF6 is not upregulated in simple steatosis [9]. One hypothesis suggests that KLF6 is upregulated in part by oxidative stress. Cardiac muscle cells treated with $H_2O_2$ had increased transcription of KLF6 [83]. Furthermore, HepG2 cells that overexpress CYP2E1 generated $H_2O_2$ and $O_2$• and had greater transcription of KLF6 when compared to control HepG2 cells. Incubation of the CYP2E1-overexpressing cells with the CYP2E1 substrate arachidonic acid increased KLF6 expression, while increased KLF6 was not observed

when arachidonic acid was added in addition to vitamin E [84]. Taken together, these data suggest that oxidative stress may be a mediator of KLF6 expression.

### *2.6 High-Fat Diet-Induced Models of NASH and Fibrosis*

When a HFD using lard as its fat source was used in a long term study of 48 wk, animals developed NASH that progressed into fibrosis [18]. Sprague Dawley rats were fed a HFD containing 30% energy from fat from lard and the control group was fed a lower-fat diet containing 10% energy from fat from lard. At week 4, rats in the 30% group developed hepatic steatosis and had greater liver mass compared to the control rats. At week 8, the rats fed 30% fat had elevated body mass, epididymal fat mass, serum free fatty acids, and serum protein concentration of TNF-α. At week 12, rats in the 30% group had histological evidence of inflammation and perisinusoidal fibrosis in addition to immunohistological staining of α-SMA and TGFβ1. At this time point, increased serum total cholesterol and serum ALT were also observed in the 30% fat group. After week 24, all of the rats had developed fibrosis which continued to develop through week 48 [18]. This study confirms that a high-fat high-lard diet induces NASH and fibrosis and that this begins around week 12 of the dietary intervention.

The aforementioned study provides a detailed framework for what occurs in an animal model fed a diet containing 30% energy from fat over an extensive period of 48 weeks. Other researchers have experimented with different fat percentages and shorter study durations [17, 85, 86]. Several studies using different diet compositions have been completed using a 12-week time frame. Sprague Dawley rats were fed either a diet containing 10% energy from fat or a diet containing 30% energy from fat as lard for 12 wk. The animals in the 30% group had an elevated number of Kupffer cells, indicating

greater inflammation. Perisinusoidal fibrosis was also observed, suggesting early stages of fibrosis [17] and these findings are consistent with the observation of Xu et al [18] described above. Mice fed a diet of 45% energy from fat as lard compared to diet of 10% energy from fat as lard for 12 wk had greater body mass, homeostatic model of insulin resistance (HOMA-IR), plasma ALT, plasma leptin and plasma free fatty acids. They also accumulated hepatic triglycerides and had histological evidence of steatosis. This study did not report on any parameters of fibrosis [85]. An even shorter study duration of 8 wk comparing a diet of 10% energy from fat as lard to one of 60% energy from fat as lard found that mice fed 60% fat diet had increased body mass, adipose mass, plasma TG, plasma free fatty acids, plasma cholesterol and plasma ALT. Additionally, there was an elevation in hepatic TGs and hepatic free fatty acids and no data was reported regarding fibrosis [86]. Taken together, these studies confirm that diets with energy percentage of 30% or greater fed over a period of 12 weeks or less can also induce oxidative stress, inflammation, NASH and, as some authors report, fibrosis.

Previous work in the model used in this thesis indicates that feeding rats a 60% fat diet for 8 weeks results in increased body mass, adipose tissue mass, serum AST, serum ALT, serum leptin and HOMA-IR compared to the low-fat diet control fed a diet of 10% energy from fat [13, 87]. Rats fed the 60% fat also had greater hepatic triglycerides, hepatic total lipids greater expression of pro-inflammatory cytokines and reduced hepatic total glutathione (tGSH) compared to the control [13], suggesting that this diet model develops NASH. Because similar diet interventions over 12 weeks have similar results with lower fat percentages and develop fibrosis, it was hypothesized that the model used by Park et al [13] would also develop fibrosis.

### *2.7 Green Tea*

At present, there is no validated treatment for NAFLD. Weight loss and co-morbidity management and lifestyle modification can be effective [5], but these interventions have poor long-term adherence [6]. This necessitates the identification of both a simple and effective therapy aimed at preventing the progression of this disease.

Several studies have indicated that green tea consumption has important mitigating effects on the components of metabolic syndrome [15, 16, 88-90] and because the development of NAFLD is closely associated with components of metabolic syndrome, GTE may exhibit protective effects against NAFLD. In a randomized, double-blind, placebo-controlled study, obese individuals having a BMI > 30 $kg/m^2$ and without hypertension, diabetes, impaired glucose tolerance or a history of coronary artery disease, stroke or abnormal liver function were provided with a 379 mg GTE supplement or a placebo. After 3 months, patients in the green tea supplement group had significantly lower total cholesterol, serum triglycerides, low-density lipoprotein cholesterol and blood glucose compared to baseline. They also had significantly greater high-density lipoprotein cholesterol and blood total antioxidant status. Compared to the placebo group, patients given the GTE supplement had reduced BMI, waist circumference, total cholesterol and low-density lipoprotein cholesterol and had greater blood total antioxidant capacity [88] This study indicates that GTE can mitigate dyslipidemia and hyperglycemia associated with obesity, promote weight loss and improve systemic antioxidant status. Epidemiological studies also suggest that green tea may have important health-promoting properties. In a study of 13,000 Japanese adults, daily consumption of one cup of green tea was associated with a reduction in serum total

cholesterol [89]. Individuals consuming >6 cups per day of green tea were less likely to develop type II diabetes than those who drank <1 cup per day per wk [90] and consumption of green tea has been shown to be inversely associated with all-cause mortality and mortality due to cardiovascular disease [15]. Increased green tea consumption has also been shown to be associated with decreased serum triglycerides, increased high-density lipoprotein cholesterol and decreased low-density lipoprotein cholesterol [16]. Furthermore, the hypothesis that GTE may have hepatoprotective properties is supported by a cross-sectional study of 1,371 Japanese men in which consumption of >10 cups/day of green tea was associated with lower serum transaminases and thus decreased liver injury [16].

*2.7.1 Green Tea Composition and Bioavailability*

To analyze the hepatoprotective effects of the entire profile of green tea components, GTE is utilized. GTE is prepared from green tea infusion and contains four major catechins, epigallocatechin gallate (EGCG), epigallocatechin (EGC), epicatechin gallate (ECG) and epicatechin (EC). These catechins represent 30–42% of the solid weight of brewed tea [91]. Catechin composition of GTE is distributed as 48% EGCG, 31% EGC, 13% ECG and 8% EC [92]. Green tea also contains the flavonols kaempferol, quercitin, and myricitin and together they comprise between 0.5% - 2.5% of the solid weight of GTE [91]. GTE also contains between 2.5-4.5% caffeine by weight [93]. GTE can be purchased in powdered form which allows it to be mixed into animal diets without altering energy consumption [13].

Consumption of GTE was chosen over EGCG or intraperitoneal injection of catechins because of the differential bioavailability of green tea catechins. A

pharmacokinetic study analyzed plasma levels of EGCG, EGC and EC in 8 subjects. Subject were administered a single oral dose 20 mg/kg body weight of green tea solids dissolved in 200 ml water on three separate occasions. GTE contained 13.9% EGCG, 11.0% EGCG and 3.2% EC by weight. The maximum plasma concentration of free plus conjugated catechins ($\pm$ standard deviation) for EGCG were 77.9 $\pm$ 22.2 ng/ml, for EGC it was 223.4 $\pm$ 35.2 mg/ml and for EC it was 124.03 $\pm$ 7.86 ng/ml. These values were observed between 1.3-1.6 h post ingestion. In the plasma, EGCG was mostly present in its free form, whereas EGC and EC were mostly in the glucuronidated conjugated form. Over 90% of the total urinary EGC and EC, almost all in the conjugated forms, were excreted after 8 hr. The quantity of 4-*O*-methyl EGC at levels higher than EGC was detected in the urine and plasma, indicating the use of this catechin as a substrate by catechol-*O*-methyl transferase [94]. This study indicates that the bioavailability of green tea catechins does not mirror the quantity ingested. EGCG was the most prevalent catechin in the GTE but it had the lowest peak plasma concentration. It also indicates that EGC and EC are more susceptible to phase II metabolism. These results should be considered when performing or interpreting experiments on isolated catechins of green tea and support the use of whole GTE in studies aiming to elucidate potential health benefits of increased green tea consumption. For this reason, this thesis investigated the effects of consuming GTE orally.

*2.7.2 Green Tea and Steatosis*

Previous work in our lab has shown that GTE can prevent the development of simple steatosis [95]. *Ob/ob* mice were fed a diet containing 0%, 1% or 2% GTE for 6 wk. Animals fed either dose of GTE had less adipose mass, lower serum transaminases

and reduced plasma and hepatic triglycerides compared to the *ob/ob* control, and GTE dose-dependently decreased hepatic total lipids and mitigated histological evidence of hepatic steatosis [95]. In another study, *ob/ob* mice were provided a diet containing 0%, 0.5% or 1% GTE for 6 wk [96]. It was observed that GTE at 1% reduced hepatic lipid content and serum free fatty acids. GTE also attenuated mRNA expression of SREBP-1c, fatty acid synthase, stearoyl-coA desaturase and hormone sensitive lipase in adipose tissue that was otherwise elevated in the *ob/ob* control. These data suggest that GTE suppresses adipose lipogenensis associated with SREBP-1c and lipolysis by hormone sensitive lipase, thereby decreasing adipose-derived free fatty acids available to the liver [96]. By reducing steatosis, the liver will be less susceptible to the lipid peroxidation and hepatocyte apoptosis, which are both initiators of fibrogenesis. Thus, by decreasing steatosis, GTE may reduce fibrosis.

Green tea catechins may exert lipid-lowering effects by increasing lipid excretion from the intestines. EGCG increases the size of the mixed micelle, which may be due to the hydroxyl moieties on EGCG forming hydrogen bonds with phosphatidyl choline molecules on different micelles which causes them to coalesce. The larger micelles then have a decreased ability to be absorbed in the intestines [97]. EGCG has also been shown to interrupt pancreatic lipase activity and phospholipase A2 activity, which also decreases intestinal lipid absorption [98]. Decreased lipid absorption means less excess energy is absorbed by the body and through this mechanism green tea may reduce steatosis.

The anti-steatotic effect of green tea may also be attributed to caffeine content [99]. When rats were infused intraduodenally with EGCG in the equivalent of consuming tea brewed from 6g of tea leaves, caffeine in the equivalent of 2 cups of coffee, or EGCG

plus caffeine, rats in either group that contained caffeine had reduced intestinal lipid absorption [99].

GTE may also mitigate steatosis by directly increasing thermogenesis [100, 101]. Intact brown adipose tissue treated with caffeine *in vitro* used oxygen at a greater rate than the control tissue. Tissue treated with EGCG and caffeine used more oxygen than the caffeine group alone [100]. This suggests that green tea catechins and caffeine promote thermogenesis through unique pathways, supporting the use of green tea to mitigate obesity through increased energy expenditure. Human studies also support the role of GTE in increasing thermogenesis. When 10 participants were provided with 90 mg catechins in addition to 50 mg of caffeine they had significantly higher resting energy expenditure over 24 hr compared to the trial in which they were provided a placebo. When they were provided with 50 mg of caffeine alone, the increase in resting energy expenditure was not observed [101].

*2.7.3 Green Tea and Oxidative Stress*

GTE also alleviates oxidative stress in the liver. *Ob/ob* mice fed a diet containing 0.5% or 1% GTE for 6 wk had decreased hepatic MDA and tGSH compared to the *ob/ob* control group. They also had increased hepatic Mn- and Cu/Zn-superoxide dismutase activity in addition to increased hepatic catalase and glutathione (GSH) peroxidase activity [96]. Additionally, Wistar rats fed a diet containing 60% energy from fat for 8 wk had significantly lower hepatic GSH and tGSH compared to the low-fat diet-fed control. Consuming the HFD in addition to 1% or 2% GTE resulted in a near dose-dependent increase in GSH and tGSH. Together, these studies suggest that GTE alleviates oxidative stress by maintaining endogenous antioxidant defenses [13].

GTE may maintain endogenous antioxidant defenses by increasing *de novo* GSH synthesis. When EGCG and buthionine sulfoximine, an inhibitor of the rate limiting enzyme in GSH synthesis glutamate-cysteine ligase (GCL), were incubated with HSCs, the GSH-raising effect of EGCG was abrogated. This suggests that the antioxidant function of EGCG requires *de novo* synthesis of GSH [102]. Supporting this hypothesis, EGCG increases GCL activity in activated HSCs by inducing greater gene expression of the catalytic subunit of GCL, GCLc [103]. GTE has also been shown to increase GCLc *in vivo* [96]. *Ob/ob* mice had lower hepatic GSH concentration compared to the lean control while there was no change in GCLc expression between obese and lean groups. This suggests that steatosis reduces hepatic GSH by increasing oxidative stress and not by inhibiting GSH biosynthesis. When *ob/ob* mice were fed a diet containing 1% GTE they had significantly greater hepatic GSH concentration than the *ob/ob* control and the increase in GSH was accompanied by increased expression GCLc to levels significantly higher than the obese control or the lean littermates [96]. These data suggest that green tea exerts it antioxidant function by modulating the expression of the rate-limiting enzyme GCL in GSH synthesis. Since oxidative stress plays an integral role in the development of fibrosis, it is possible that GTE protects against fibrosis by upregulating GSH.

Furthermore, GTE has been shown to upregulate other endogenous antioxidant defense enzymes. Ob/ob mice consuming 1% GTE had significantly greater Mn-superoxide dismutase, Cu/Zn-superoxide dismutase activity, GSH peroxidase and catalase activity compared to obese controls [96]. Similar effects were observed in Wistar rats that were intragastrically administered 1.8 ml ethanol every day for 4 wk and

provided with water containing 3 g/L GTE. Rats in the ethanol plus green tea group had significantly greater hepatic levels of Cu/Zn-dismutase, GSH peroxidase and catalase compared to the group administered ethanol without access to green tea [104]. This indicates that GTE increases other antioxidant defenses in addition increasing *de novo* synthesis of GSH.

*2.7.4 Green Tea and Inflammation*

Green tea also has anti-inflammatory properties [13, 105]. Sprague Dawley rats provided a diet containing 0.1% GTE 5 days prior to ischemia-reperfusion surgery had less liver injury and lower mononuclear cell infiltration 24 hr post-surgery compared to the positive control [105]. Animals fed GTE also had lower hepatic nuclear NFκB/DNA complexes and lower hepatic and plasma TNF-α mRNA [105]. Wistar rats fed a diet containing 60% energy from fat for 8 wk developed steatosis and liver injury, however, when 1% or 2% GTE was provided in addition to the HFD, animals had less steatosis as well as decreased NFκB binding activity in adipose and liver tissue. The decrease in NFκB was accompanied by a decrease in downstream expression of MCP-1 and TNF-α in both tissues [13].

The mechanism by which this occurs may be dependent on the antioxidant activity of GTE. NFκB is a redox-sensitive transcription factor responsible for transcription of TNF-α [64] and MCP-1 [63] that is activated by oxidative stress [106] and it is inhibited by the oxidant-scavenging effects of enzymes such as GSH peroxidase and Mn-superoxide dismutase [107]. As mentioned previously, GTE improves hepatic antioxidant status and augments the activity of these antioxidant enzymes. This may lead

to decreased transcription of downstreatm target genes of NFκB that promote inflammation.

GTE may also protect against oxidative damage associated with inflammation by reducing inflammatory cell infiltration. Apoptotic hepatocytes release pro-inflammatory mediators, which attracts Kupffer cells and neutrophils [1]. In an inflammatory environment, these cells produce ROS with the enzymes NADPH-oxidase and myeloperoxidase [50]. *Ob/ob* mice fed a diet containing 1% GTE had less myeloperoxidase protein expression and less NADPH-oxidase activity than the obese control [108], indicating that GTE can mitigate inflammatory cell infiltration.

GTE may also protect against inflammation mediated by prostaglandin$E_2$ [87]. The enzyme cyclooxygenase-2 is upregulated by NKκB [109] and generates prostaglandin$E_2$ [110]. Prostaglandin$E_2$ binding to its receptor then potentiates the innate immune response [110]. Rats fed a HFD for 8 wk in addition to 2% GTE had reduced protein levels and activity of cyclooxygenase-2 as well as less hepatic prostaglandin$E_2$ [87], indicating that GTE may prevent inflammation induced by this pathway.

*2.7.5 Green Tea and Fibrosis*

Several studies have been completed in animals that indicate the anti-fibrogenic property of GTE [111-113]. Sprague Dawley rats injected intraperitoneally with a single dose of 500 mg/kg galactosamine to induce hepatocyte apoptosis and inflammation and provided with a green tea beverage (17 mg/kg/day GTE) had lower serum AST and ALT at 24 h post-injection compared to the positive control. Animals also had lower procollagen(α1)I and TGFβ1 mRNA after 24 hr. After 14 days, there was significantly less staining for collagen in hepatic tissue from the GTE treatment group compared to the

positive control [111]. Sprague Dawley rats fed a diet containing 0.1% GTE beginning 3 days prior to bile-duct ligation surgery had less liver injury after 24 hr compared to the bile-duct ligation control, while after 3 wk animals fed the GTE diet had less fibrosis, reduced immunohistochemical staining for α-SMA and reduced hepatic procollagen(α1)I mRNA compared to the positive control. The GTE group also had less nuclear NFκB/DNA and AP-1/DNA complexes as well as reduced TGFβ1 and TNF-α mRNA [112]. Wistar rats injected with 0.5 ml/kg/day $CCl_4$ in addition to being provided daily with water containing 0.1% EGCG had lower serum transaminases, less histological staining of collagen and lower hepatic hydroxyproline concentration as well as lower protein levels of α-SMA compared to the control group. The 0.1% EGCG treatment also resulted in lower message level and protein expression of PDGF-Rβ [113]. These studies indicate that oral consumption of GTE also has antifibrogenic properties.

Green tea may prevent fibrosis by decreasing activity of NFκB. The studies summarized above indicate that GTE and EGCG reduce hepatic NFκB binding activity. NFκB promotes transcription of PDGF-Rβ [114] which promotes HSC proliferation [68]. NFκB also upregulates transcription of AGE-receptors [115], which upon AGE binding leads to increased HSC activation [74]. NFκB also initiates transcription of TNF-α which has an important roles in insulin resistance [28] and apoptosis [49]. Thus, by decreasing NFκB binding activity, GTE may protect against fibrosis through various pathways.

Decreased TGFβ1 signaling may be another mechanism by which GTE may protect against fibrosis. TGFβ1 increases expression of the procollagen(α1)I gene in HSCs by promoting the formation of $H_2O_2$, which stimulates expression of C/EBPβ and promotes binding of this factor to a TGFβ1-responsive element located in the

procollagen(α1)I gene promoter [66]. Since GSH peroxidase is responsible for detoxifying intracellular $H_2O_2$ and GTE increases GSH peroxidase activity in animals with NAFLD [96], it is possible that GTE disrupt procollagen(α1)I transcription by increasing GSH peroxidase.

Another mechanism by which GTE may protect against fibrosis is by preventing leptin resistance, since elevated circulating leptin is associated with advanced NAFLD [116]. As mentioned previously, leptin has been shown to play an integral role in fibrosis by increasing levels of free TGFβ1 [75], promoting further leptin expression by HSCs [76] and by promoting HSC proliferation [77]. Rats fed a diet containing 60% energy from fat had increased serum leptin compared to animals fed a diet containing 10% energy from fat. When rats were fed the 60% diet in addition to 1% or 2% GTE, they had significantly reduced levels of serum leptin [13]. Thus, it is possible that by modulating levels of circulating leptin, GTE prevents fibrosis.

### *2.8 Conclusion*

All of these studies indicate that green tea has health-promoting properties that are hepatoprotective by many mechanisms. Evidence from several models and several doses of GTE has shown that GTE can mitigate steatosis, inflammation and oxidative stress. What is missing from the literature is a HFD-induced obese model that replicates the symptoms of obesity and exhibits disease progression of NASH into fibrosis. For that reason we have used a HFD-induced model of NALFD to examine the effect of GTE on fibrogenesis.

**Figure 2.1** *Examples of Liver Histology*

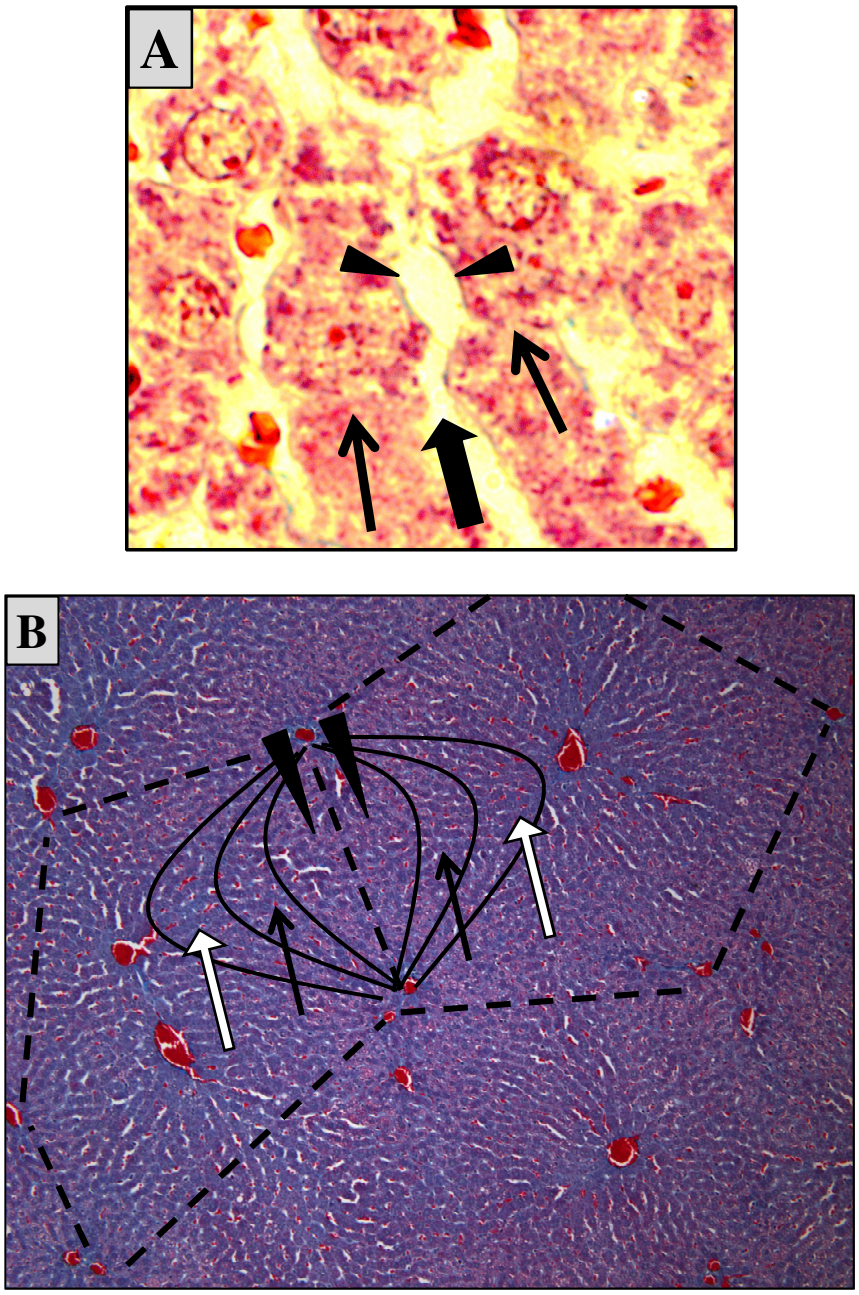


A) Liver tissue, 100×. Thick black arrow indicates sinusoidal space. Thin black arrow indicates a cord of hepatocytes. Black wedges indicate space of Disse. B) Structure of the liver lobule and identification of the acinar zones, 10×. Dotted lines show separation between lobules. Solid curves indicate zonal separation. Black wedges indicate zone 1 of the liver acinus. Black arrows indicate zone 2. White arrows with black borders indicate zone 3.

# Chapter 3: Materials and Methods

### *3.1 Materials*

All chemicals used for hydroxyproline determination and western blotting were purchased from Fisher Scientific (Waltham, MA). Dried nonfat milk was purchased from Big Y Foods, Inc. (Springfield, MA). Western blotting for α-SMA was performed using the Criterion Cell for electrophoresis (#165-6001, Bio-Rad, Hercules, CA) and the Criterion Blotter with Wire Electrodes for transfer (#170-4071, Bio-Rad, Hercules, CA). Western blotting for KLF6 was performed using the Criterion Cell for electrophoresis (#165-6001, Bio-Rad, Hercules, CA) and the Criterion Blotter with Plate Electrodes for transfer (#170-4070, Bio-Rad, Hercules, CA).

### *3.2 Study Design*

The design for this study has been reported previously [13] and is summarized below. The study protocol was approved by the Institutional Animal Care and Use Committee at the University of Connecticut. Male Wistar rats (n = 63; 16 wk old) were purchased from Harlan Laboratories and housed individually in an environmentally controlled room with a 12 h light-dark cycle. After 1 wk of acclimation, rats were randomly assigned to 1 of 4 dietary groups for 8 wk: a low-fat diet (LFD) group containing no GTE, a HFD group containing no GTE, a HFD containing GTE at 1% (wt:wt) (HFD+1% GTE) group, or a HFD containing 2% GTE (HF+2% GTE) group. The LFD contained 10% energy from lard and 70% energy from carbohydrates while the HFD contained 60% energy from lard and 20% energy from carbohydrates. The diets both had 20% energy from protein (**Table 3.1**). Powdered GTE containing 30% (wt:wt) total catechins [95] was provided by Unilever BestFoods (Englewood Cliffs, NJ) and was

mixed into the HFD. GTE at 1% or 2% was chosen because on the basis of energy intake. 1% and 2% GTE are estimated to be equivalent to 7 and 14 servings/d of green tea in humans [95] where a serving of green tea is approximately 120 ml, which is common in certain part of the world [15, 117]. These levels are consistent with epidemiologic findings suggesting that green tea consumed at ~10 servings/d may be related to lower levels of liver injury [16] and evidence from our previous studies show that these levels of GTE attenuate hepatic steatosis and injury in genetically obese mice [95]. After 8 wk of feeding, rats were killed under isoflurane anesthesia following 10–12 h of food deprivation. Liver was harvested, snap-frozen in liquid nitrogen, and stored at -80°C. Portions of liver were formalin fixed and embedded in paraffin for histological analysis. Hydroxyproline concentration, α-SMA protein expression and KLF6 nuclear protein expression were then determined.

### *3.3 Determination of Perisinusoidal Fibrosis*

Tissue sections were deparaffinized and rehydrated using the following protocol: immersion in xylene for 3 min followed by immersion in xylene again for 3 min, immersion in 50% xylene in ethanol for 3 min, immersion in 100% ethanol for 3 min, immersion in 100% ethanol for 3 min, immersion in 95% ethanol for 3 min, immersion in 70 % ethanol for 3 min and immersion in 50 % ethanol for 3 min. Slides were then rinsed under cold water and placed in Bouin's fixative solution (#S129 Poly Scientific R&D, Bay Shore, NY) overnight at room temperature and rinsed with distilled water until the sections were colorless. Slides were placed in Weigert's iron hematoxylin stain (#S216B, Poly Scientific R&D, Bay Shore, NY) for 10 min and subsequently rinsed with distilled water until clear. Slides were then placed in Gomori's 1-step trichrome stain (#S1816,

Poly Scientific R&D, Bay Shore, NY) for 15 min, then rinsed with water until clear, then subsequently placed in 5% acetic acid for 2 min. Slides were then placed 95% ethanol for 1 min followed by placement in 100% ethanol for 1 min then placement in xylene for 1 min then covered with synthetic resin and coverslip. Images (100×) from the perisinusoidal area between the central vein and the portal triads were captured using an Olympus IX70 (Olympus, Center Valley, PA) inverted microscope with accompanying software (DP2-BSW Version 2.2, Olympus, Center Valley, PA).

### *3.4 Hydroxyproline*

Hydroxyproline concentration was determined using the method described by Reddy et al [118] with modifications. Liver (~0.2 g) was weighed and homogenized in 5 vol of 0.9% NaCl in water using an Omni General Laboratory Homogenizer (#GLH-155, Omni International, Kennesaw, GA). Liver homogenate or hydroxyproline standard (**Table 3.2A**) (40 µL) were added to locking microcentrifuge tubes, followed by 10 µL of 10 M NaOH. Samples were then autoclaved for 20 min at 120°C. After cooling to room temperature, 0.056 M chloramine-T solution (**Table 3.2B**) (450 µL) was added. Samples were then incubated at room temperature for 25 min, after which Ehrlich's reagent (**Table 3.2C**) (500 µL) was added. Samples were vortexed briefly and heated in a water bath at 65°C for 20 min to develop the chromophore pyrrole-2-carboxylic acid from hydroxyproline and *para*-dimethylaminobenzaldehyde. 200 µL of each sample were loaded onto a 96 well plate, placed in the spectrophotometer (SpectraMax M2, Molecular Devices, Sunnyvale, CA) and optical density was measured at 550 nm. Linear regression between hydroxyproline concentration and optical density was performed to generate a

standard curve of known hydroxyproline concentrations. Data was reported as ug/g tissue as there was no change in liver mass between groups [13].

### *3.5 α-Smooth Muscle Actin*

Liver (~0.2 g) was weighed and homogenized 1:5 (wt/wvol) using radioimmunoprecipitation assay (RIPA) buffer (**Table 3.3A**) containing protease inhibitor cocktail (PIC) and EDTA (#78430, Pierce Biotechnology, Rockford, IL) in a 1:100 ratio for each the PIC and 0.5 M EDTA provided in the kit. Tissue was then homogenized over ice for 10 sec using an Omni General Laboratory Homogenizer (#GLH-155, Omni International, Kennesaw, GA). Samples were aliquoted into microcentrifuge tubes and centrifuged at 1,000 g for 10 min. The supernatant was removed and stored at -80°C until needed.

To determine the protein concentration of samples, homogenized tissue samples were centrifuged at 1,000 g for 5 min and 1:100 dilutions were prepared. Protein concentration was then determined using the Thermo Scientific Pierce BCA Protein Assay Kit (#23227, Pierce Biotechnology, Rockford, IL) according to the manufacturer's instructions. Linear regression between protein concentration and optical density was performed to generate a standard curve of known protein concentrations. The BCA assay for protein determination is based on the principle that the addition of the working reagent to any sample containing protein will cause peptides containing 3 or more amino acids to form a colored chelate complex with cupric ions. Bicinchoninic acid (BCA) reacts with the cupric cations formed from the addition of working reagent and develops into an intense purple-colored reaction product which results from the chelation of 2

molecules of BCA with 1 cuprous ion. The newly formed BCA/copper complex exhibits a strong linear absorbance at 562 nm with increasing protein concentrations.

For electrophoresis, a 4-16% gradient gel was cast using a gradient gel former (#165-4120, Bio-Rad, Hercules, CA). polyacrylamide solutions (4% and 16%) were prepared simultaneously but independently. Purified water, 1.5 M Tris-HCL (pH 8.8), 20% sodium dodecyl sulfate (SDS), 30% acrylamide/bis-acrylamide solution (#161-0158, Bio-Rad, Hercules, CA), tetramethylethylenediamine (TEMED) and 10% ammonium persulfate (APS) were combined in the appropriate volumes (**Table 3.3B**) and mixed thoroughly. The solutions were then added to individual columns of the gradient gel former. The solutions were then pumped out of the gradient gel formers and added to a Bio-Rad Criterion 26 well empty cassette (#345-9903, Bio-Rad, Hercules, CA), stopping the flow of gel solution ~50 mm below the well markings. 100% butanol (~3 ml) was added to the cassette and the gel was allowed to solidify for 60 min. After 60 min, the butanol was decanted and the surface of the gel was washed with deionized water and then dried with filter paper. While the running gel was solidifying, the same protocol as above was performed for the stacking gel except that 0.5 Tris-HCL (pH 6.8) was substituted for 1.5 M Tris-HCl (pH 8.8). After the gradient gel was solidified, the stacking gel solution (~ 3 ml) was pipetted to completely fill the cassette and then the 26 well comb was inserted. After 30 min the gel was ready to be used for western blotting or stored in moistened paper towels in a plastic bag at 4°C until needed.

To prepare samples for electrophoresis, homogenized samples were centrifuged at 1,000 g for 5 min. Using the protein concentrations calculated in the previous step, the volume containing 100 ug of protein was removed from each sample and added to

locking microcentrifuge tubes. The volume was adjusted to a total volume of 15 μL with distilled water followed by the addition of 5 μL of 4x sample buffer (**Table 3.3C**). Samples were vortexed and placed in a 95°C water bath for 10 min and centrifuged at 1,000 g for 60 sec.

Samples and protein standard (#161-0374, Bio-Rad, Hercules, CA) were loaded onto the 4%-16% polyacrylamide gradient gel and run in running buffer (**Table 3.3D**) at 20 V for 30 min followed by 100V for 60 min. Proteins were transferred in transfer buffer (**Table 3.3E**) to PVDF (#162-0177, Bio-Rad, Hercules, CA) for 60 min at 330 milliamps. Prior to transfer, the PVDF membrane was incubated in methanol on a rocking platform for 2 min. Methanol was removed and PVDF was then incubated with transfer buffer for another 2 min. After transfer, the membrane was blocked in blocking buffer (**Table 3.3F**) for 15 min at room temperature. The membrane was then incubated with rabbit anti-α-SMA antibody (#sc-130619, Santa Cruz Biotechnology, Santa Cruz, CA) diluted 1:500 in blocking buffer overnight at room temperature. The membrane was then washed 3 times in TBS-T (Tris Buffered Saline-Tween 20) (**Table 3.3G**) on a rocking platform for 5 min each. The membrane was incubated in horseradish peroxidase (HRP)-conjugated anti-rabbit secondary antibody (#sc-2004, Santa Cruz Biotechnology, Santa Cruz, CA) diluted 1:5000 in blocking buffer for 60 min at room temperature, followed by 3 more washings in TBS-T for 5 min each. The membrane was then incubated with Pierce ECL Western Blotting Substrate (#PI-32106, Pierce Biotechnology, Rockford, IL) and developed with a Bio-Rad ChemiDoc XRS+ System (Bio-Rad, Hercules, CA). Band density was then analyzed with the accompanying software (Image Lab version 4.0, Bio-Rad, Hercules, CA).

After developing, the membrane was washed for 5 min in deionized water. Then 0.4 N NaOH was added to the membrane for 5 min, followed by washing in deionized water for 5 min. The membrane was then blocked for 15 min at room temperature in blocking buffer.

To control for protein loading, the membrane was then incubated with mouse anti-β-tubulin antibody (#sc-58886, Santa Cruz Biotechnology, Santa Cruz, CA) diluted 1:500 in blocking buffer for 60 min. Membrane was then washed 3 times for 5 min in TBST-T and incubated with HRP-conjugated anti-mouse secondary antibody (#sc-2005, Santa Cruz Biotechnology, Santa Cruz, CA) diluted 1:5000 in blocking buffer for 60 min. The membrane was washed 3 times for 5 min in TBS-T and incubated with Pierce ECL Western Blotting Substrate (#PI-32109, Pierce Biotechnology, Rockford, IL) and developed with a Bio-Rad ChemiDoc XRS+ System (Bio-Rad, Hercules, CA). Band density was then analyzed with the accompanying software (Image Lab version 4.0, Bio-Rad, Hercules, CA).

### *3.6 Kruppel-like Factor 6*

Isolation of the nuclear fraction from liver tissue was performed using the Thermo Scientific NE-PER Nuclear and Cytoplasmic Extraction Kit (#78835, Pierce Biotechnology, Rockford, IL) according to the manufacturer's instructions with modifications. Cytoplasmic Extraction Reagent I (CER I) and Nuclear Extraction Reagent (NER) were prepared with Thermo Scientific Protease Inhibitor Cocktail (PIC) and EDTA (#78430, Pierce Biotechnology, Rockford, IL) in the ratio of 1:100 for each the PIC and 0.5 M EDTA, both of which were provided by in the kit. PIC and EDTA were added to prevent digestion of protein by endogenous proteases and

metalloproteinases. Tissue (~55 mg) was homogenized 1:10 (wt/wvol) in CER I using an Omni General Laboratory Homogenizer (#GLH-155, Omni International, Kennesaw, GA) to cause swelling of cellular membranes. Homogenized sample (500 µL) was then aliquoted into microcentrifuge tubes. CER II (27.5 µL) was added to lyse cell membranes, allowing cytoplasmic proteins to be collected, while leaving the nucleus intact. Each sample was then vortexed for 5 sec. After 1 min of incubating on ice, samples were vortexed again for 5 sec and centrifuged at 16,000 g for 5 min at 4°C to pellet the nuclear fraction. Supernatant was then removed and stored as the cytoplasmic fraction. NER + PIC & EDTA (62.5 µL) was then added to the pellet to lyse the nuclear fraction and samples were vortexed for 15 sec. After incubation on ice for 10 min, samples were again vortexed for 15 sec. This was repeated 3 more times for a total of 40 min. Samples were then centrifuged for 10 min at 16,000 g at 4°C. Supernatant was removed and stored as the nuclear fraction.

After nuclear extraction, 1:10 dilutions of each nuclear fraction sample were prepared. Sample protein concentration was then determined using the Thermo Scientific Pierce BCA Protein Assay Kit (#23227, Pierce Biotechnology, Rockford, IL) according to the manufacturer's instructions and according to the principle described above.

Using the protein concentrations determined from the BCA assay, the volume of sample containing 50 ug was removed from nuclear extract stocks and added to locking microcentrifuge tubes. The volume was adjusted to 15 µL with distilled water followed by the addition of 5 µL of 4x sample buffer. Samples were vortexed and placed in a 95°C water bath for 10 min and centrifuged at 1,000 g for 60 sec.

For electrophoresis, a 10% polyacrylamide slab gels were prepared. For the running gel, purified water, 1.5 M Tris-HCl (pH 8.8), 20% SDS and 30% acrylamide/bis-acrylamide solution, TEMED and 10% APS were combined in the appropriate volumes (**Table 3.3B)** and mixed thoroughly. The solution (~13 ml) was then pipetted gently into a Bio-Rad Criterion 26 well empty cassette (#345-9903, Bio-Rad, Hercules, CA) until ~50 mm below the well markings. 100% butanol (~3 ml) was then pipetted into the cassette. After 60 min, the butanol was decanted and the surface of the gel was washed gently with deionized water then dried with filter paper. While the running gel was solidifying, the same protocol as above was performed for the stacking gel except that 1.5 M Tris-HCl (pH 8.8) was replaced with 0.5 M Tris-HCL (pH 6.8). The stacking gel solution (~3 ml) was then pipetted into the cassette until full and then the 26 well comb was inserted. After 30 min the gel was ready to be utilized for electrophoresis or stored in moistened paper towels in a plastic bag at 4°C until needed.

Samples and protein standard (#161-0374, Bio-Rad, Hercules, CA) were loaded onto the 10% slab polyacrylamide gel and run at 100 V for 90 min in running buffer. Proteins were transferred in transfer buffer to PVDF (#162-0177, Bio-Rad, Hercules, CA) for 40 min at 100 V in 4°C. Prior to transfer, the PVDF membrane was incubated in methanol on a rocking platform for 2 min. Methanol was then removed and PVDF was incubated in transfer buffer for another 2 min. After transfer, the membrane was blocked in blocking buffer for 60 min at room temperature. Incubation with rabbit anti-KLF6 antibody (#sc-7158; Santa Cruz Biotechnology, Santa Cruz, CA) diluted 1:200 in blocking buffer for 60 min at room temperature was followed by 3 washings in TBS-T for 5 min each. The membrane was incubated with HRP-conjugated anti-rabbit secondary

antibody (#162-0177, Bio-Rad, Hercules, CA) diluted 1:1000 in blocking buffer for 60 min at room temperature, followed by 3 washings in TBS-T for 5 min each. The membrane was incubated with Pierce ECL Western Blotting Substrate (#PI-32109, Pierce Biotechnology, Rockford, IL) and developed with a Bio-Rad ChemiDoc XRS+ System (Bio-Rad, Hercules, CA). Band density was then analyzed with the accompanying software (Image Lab version 4.0, Bio-Rad, Hercules, CA).

After developing, the membrane was incubated in stripping buffer (**Table 3.3H**) for 5 min. Then the buffer was replaced with new stripping buffer for another 5 min. After stripping, the membrane was washed 2 times for 10 min each in PBS, followed by washing in TBS-T 2 times for 5 min each. The membrane was then blocked at room temperature for 60 min in blocking buffer.

To control for protein loading, the membrane was incubated in mouse anti-TATA-box binding protein antibody (#AB818, Abacam, Cambridge, MA) diluted 1:10,000 diluted in blocking buffer for 2 h followed by washing 3 times for 5 min in TBST-T and incubation with HRP-conjugated anti-mouse secondary antibody diluted 1:1000 in blocking buffer for 60 min. The membrane was washed 3 times for 5 min in TBS-T and incubated with Pierce ECL Western Blotting Substrate (#PI-32109, Pierce Biotechnology, Rockford, IL) and developed with a Bio-Rad ChemiDoc XRS+ System (Bio-Rad, Hercules, CA). Band density was then analyzed with the accompanying software (Image Lab version 4.0, Bio-Rad, Hercules, CA).

### *3.7 Statistical Analysis*

Data (means ± SE) were analyzed using GraphPad Prism (Version 5.02; GraphPad Software, Inc.; San Diego, CA, USA). One-way ANOVA with Newman-

Keuls's post-test was used to evaluate the differences between group means. Regression analysis was used to evaluate associations between variables. Analyses were considered statistically significant at an $\alpha$-level of $P < 0.05$.

**Table 3.1** *Composition of Experimental Diets*[1]

| **Low Fat Diet (D12450B)** | |
|---|---|
| **Macronutrient Composition** *% Total Energy* | |
| Protein | 20 |
| Carbohydrate | 20 |
| Fat | 10 |
| **Fat Composition** *% Total Fat* | |
| Saturated | 22.7 |
| Monounsaturated | 29.9 |
| Polyunsaturated | 47.4 |
| **Ingredients** *(g/kg)* | |
| Casein | 200 |
| L-cystine | 3 |
| Corn Starch | 315 |
| Maltodextrin | 35 |
| Sucrose | 350 |
| Cellulose | 50 |
| Soybean Oil | 25 |
| Lard | 20 |
| Mineral Mix | 10 |
| DiCalcium Phosphate | 13 |
| Calcium Carbonate | 5.5 |
| Potassium Citrate | 16.5 |
| Vitamin Mix | 10 |
| Choline Bitatarate | 2 |

| **High Fat Diet (D12492)** | |
|---|---|
| **Macronutrient Composition** *% Total Energy* | |
| Protein | 20 |
| Carbohydrate | 70 |
| Fat | 60 |
| **Fat Composition** *% Total Fat* | |
| Saturated | 32.0 |
| Monounsaturated | 35.9 |
| Polyunsaturated | 32.0 |
| **Ingredients** *(g/kg)* | |
| Casein | 200 |
| L-cystine | 3 |
| Corn Starch | 0 |
| Maltodextrin | 125 |
| Sucrose | 68.8 |
| Cellulose | 50 |
| Soybean Oil | 25 |
| Lard | 245 |
| Mineral Mix | 10 |
| DiCalcium Phosphate | 13 |
| Calcium Carbonate | 5.5 |
| Potassium Citrate | 16.5 |
| Vitamin Mix | 10 |
| Choline Bitatarate | 2 |

[1]Research Diets, Inc. New Brunswick, NJ

**Table 3.2** *Reagents for Hydroxyproline Determination*

| A. Hydroxyproline Standard |
|---|
| 5 mg hydroxyproline<br>5 ml $H_2O$ |

| B. Chloramine-T Solution: |
|---|
| 0.056 M Chloramine-T trihydrate<br>10% propanol<br>Prepared in acetate-citrate buffer |

| C. Acetate-Citrate Buffer (pH 6.5): |
|---|
| 880 mM sodium acetate trihydrate<br>220 mM citric acid<br>850 mM NaOH<br>1.2% glacial acetic acid<br>Prepared in $H_2O$ |

| D. Ehrlich's Reagent: |
|---|
| 1M para-dimethylaminobenzaldehyde<br>Prepared in 2:1 n-propanol/60% perchloric acid |

**Table 3.3** *Reagents for Western Blotting*

| A. RIPA Buffer |
|---|
| 50 mM Tris-HCl, pH 7.4 |
| 150 mM NaCl |
| 0.1% SDS |
| 0.5% Sodium Deoxycholate |
| 1% NP-40 |

B. Gel Preparation

| | 4% Gel | 10% Gel | 16% Gel | Gradient Stacking Gel | Slab Stacking Gel |
|---|---|---|---|---|---|
| % Acrylamide | 4 | 10 | 16 | 3 | 5 |
| Final Volume Desired (ml) | 7 | 3.75 | 7 | 3 | 5 |
| $H_2O$ (ml) | 4.24 | 6.09 | 1.44 | 1.92 | 2.86 |
| 1.5 M Tris-HCl, pH 8.8 (ml) | 1.75 | 3.75 | 1.75 | 0 | 0 |
| 0.5 M Tris-HCl, pH 6.8 (ml) | 0 | 0 | 0 | 0.75 | 1.25 |
| 20% SDS (ml) | 0.04 | 0.08 | 0.04 | 0.015 | 0.03 |
| 30% Acrylamide/Bis (ml) | 0.93 | 5 | 3.73 | 0.3 | 0.83 |
| 10% (w/v) APS (ml) | 0.04 | .08 | 0.04 | 0.015 | 0.03 |
| TEMED (ml) | 0.004 | .01 | 0.004 | 0.003 | 0.005 |

| C. 4x Sample Buffer Stock |
|---|
| 10% SDS (w/v) |
| .25 M Tris HCl (pH 6.8) |
| 32% (v/v) glycerol |
| 0.017% bromophenol blue |

| D. Running Buffer |
|---|
| 50 mM Tris-HCl |
| 380 mM Glycine |
| 0.1% SDS |

| E. Transfer Buffer |
| --- |
| 50 mM Tris-HCl |
| 380 mM Glycine |
| 0.1% SDS |
| 10% Methanol |

| F. Blocking Buffer |
| --- |
| 5% Dry Non-fat Milk |
| Prepared in TBS-T |

| G. TBS-T |
| --- |
| 100 mM Tris-HCl |
| 0.9% NaCl |
| 0.1% Tween-20 |

| H. Stripping Buffer (pH 2.2) |
| --- |
| 200 mM Glycine |
| 3.5 mM SDS |
| 1% Tween-20 |

# Chapter 4: Results

### *4.1 Body Weight, Insulin Resistance, Liver Injury and Oxidative Stress*

The effects of GTE on body composition, energy intake, serum AST, serum ALT, tGSH, nuclear NFκB activity [13], plasma glucose levels, plasma insulin levels and insulin resistance [87] have been reported previously. In brief, after the 8 wk dietary intervention, the HFD group had 30% greater adipose mass ($P < 0.001$) and gained significantly more weight ($P < 0.01$) than the LFD group. The body weight of rats in HFD+1% GTE and HFD+2% GTE was not different than body weight of rats fed the LFD. The difference in body weight between the groups occurred without a significant change in energy intake ($P > 0.05$, **Table 4.1**). The HFD group was more insulin resistant as calculated by HOMA-IR (Glucose×Insulin/22.5) compared to the LFD group. HFD+1% GTE and HFD+2% GTE groups had HOMA-IR comparable to the LFD group (**Table 4.1**). These data support that GTE mitigates weight gain and insulin resistance, independent of any changes in energy intake. Plasma ALT in the HFD group was nearly double that of the LFD group while ALT in the HFD+GTE 1% or 2% was similar to the LFD group. ($P <0.0001$, **Table 4.1**). The HFD group also had nearly double plasma AST levels compared to the LFD group. The HFD+GTE 1% group had 18% lower plasma AST and the HFD+GTE 2% group had 32% lower AST compared to HFD ($P = 0.001$, **Table 4.1**). The HFD group had 32% lower concentrations of tGSH compared to the LFD group. GTE treatment near dose-dependently increased tGSH to the extent that tGSH in the HFD+GTE 2% group was significantly higher than the HFD group ($P<0.0001$, **Table 4.1**).

### *4.2 Perisinusoidal Fibrosis and Hepatic Hydroxyproline*

Hepatic fibrosis resulting from NAFLD begins in the perisinusoidal area between the hepatic cords [25] (**Figure 2.5.1A**). Visualization of liver sections following trichrome staining showed evidence of collagen deposition within the perisinusoidal space of rats in the HFD group, whereas rats in the LFD group as well as in the HFD+GTE 1% and HFD+2% GTE groups had less histological evidence of perisinusoidal fibrosis (**Figure 4.2.1**).

The occurrence of hydroxyproline is exclusive to connective tissue where it occupies the Y position of the glycine-X-Y repeating peptide of collagen [119]. Hepatic hydroxyproline concentrations were higher in the HFD group compared to the LFD group ($P < 0.05$, **Figure 4.2.2**). HFD+1% GTE and HFD+2% GTE groups had less hydroxyproline than the HFD group and had hydroxyproline not different than the LFD group. Thus, GTE prevents hepatic fibrosis and mitigates hepatic collagen accumulation in HFD-induced NAFLD. Serum AST released by damaged hepatocytes has been identified as an indicator of the extent of hepatic fibrosis [26]. Regression analysis of AST and hepatic hydroxyproline indicates that AST positively correlated with hepatic hydroxyproline concentrations ($r = 0.30$, $P < 0.05$, **Figure 4.2.3A**), suggesting that hepatocyte injury is associated with hepatic collagen deposition. Additionally, tGSH was inversely correlated with hepatic hydroxyproline concentrations ($r = -0.33$, $P = 0.01$, **Figure 4.2.3B**), suggesting that greater oxidative stress results in greater hepatic collagen deposition.

### *4.3 Hepatic α-SMA*

Rats fed the HFD had 37% greater hepatic α-SMA expression compared to the LFD group ($P < 0.01$, **Figure 4.3.1**). α-SMA expression in the HFD+1% GTE group was higher ($P < 0.01$) than that from the LFD group and not different from that of the HFD group. However, α-SMA expression of the HFD+2% GTE group was 31% less than that of the HFD group and was not statistically different from LFD group. These data indicates that greater dietary levels of GTE may mitigate HSC activation. Because HSCs deposit collagen during hepatic fibrosis [58], the correlation between α-SMA and hydroxyproline concentration was analyzed. Consistent with the etiology of hepatic fibrosis [1], α-SMA protein expression was correlated to hydroxyproline concentrations ($r = 0.43$, $P < 0.001$, **Figure 4.3.2A**). Serum AST was also correlated with α-SMA expression ($r = 0.30$, $P < 0.05$, **Figure 4.3.2B**) suggesting that greater liver injury induces greater HSC activation. Hepatic tGSH was inversely related to α-SMA expression ($r = -0.31$, $P < 0.05$, **Figure 4.3.2C**), suggesting that greater oxidative stress may promote activation of HSCs. Regression analysis also indicates that NFκB activity correlated positively ($r = 0.33$, $P < 0.05$, **Figure 4.3.2D**) with α-SMA expression, indicating that inflammation associated with greater NFκB nuclear binding activity may be associated with greater HSC activation.

### *4.4 Hepatic Nuclear KLF6*

KLF6 is a transcription factor that upregulates important fibrogenic proteins such as pro-collagen(α1)I and TGFβ1 [11] and is induced by oxidative stress [84]. Nuclear KLF6 protein was 77% higher in the HFD group compared to the LFD group (**Figure 4.4**). Nuclear protein levels of KLF6 in the HFD+1% GTE and HFD+2% GTE groups

were higher than that of the LFD group ($P < 0.01$) and were not significantly different from the HFD group. This suggests that nuclear translocation of KLF6 is unaffected by GTE.

**Table 4.1** *Body Composition, Energy Intake, and Biochemical Markers of NAFLD* from rats fed a LFD, HFD, HFD+1% GTE or HFD+ 2% GTE for 8 wk[1]

| | LFD | HFD | HF + 1% GTE | HF + 2% GTE | P |
|---|---|---|---|---|---|
| [2]**Initial Body Weight (g)** | 369.0 ± 5.1 | 373.7 ± 4.7 | 370.2 ± 4.5 | 372.3 ± 4.2 | >0.05 |
| [2]**Final Body Weight (g)** | 512.8 ± 12.4$^{a}$ | 572.2 ± 11.5$^{b}$ | 512.7 ± 13.3$^{a}$ | 537.6 ± 11.2$^{a}$ | <0.01 |
| [2]**Liver Mass (g)** | 14.1 ± 0.8 | 14.4 ± 0.3 | 13.2 ± 0.7 | 12.8 ± 0.4 | >0.05 |
| [2]**Energy Intake (kcal/d)** | 90.2 ± 2.5 | 90.8 ± 1.7 | 85.4 ± 4.2 | 86.6 ± 2.0 | >0.05 |
| [3]**Plasma Glucose (mmol/L)** | 13.4 ± 0.7 | 12.6 ± 0.9 | 11.8 ± 0.5 | 11.7 ± 0.3 | >0.05 |
| [3]**Plasma Insulin (ng/ml)** | 2.6 ± 0.3$^{a}$ | 3.7 ± 0.5$^{b}$ | 2.3 ± 0.2$^{a}$ | 2.1 ± 0.3$^{a}$ | <0.01 |
| [3]**HOMA-IR** | 34.1 ± 4.5$^{a}$ | 50.2 ± 8.3$^{b}$ | 29.6 ± 2.9$^{a}$ | 26.5 ± 4.0$^{a}$ | <0.05 |
| [2]**Serum AST (U/L)** | 54.6 ± 3.8$^{a}$ | 98.6 ± 9.9$^{b}$ | 80.7 ± 7.5$^{bc}$ | 67.1 ± 4.8$^{ac}$ | <0.001 |
| [2]**Serum ALT (U/L)** | 28.8 ± 2.3$^{a}$ | 57.1 ±7.2$^{b}$ | 35.5 ± 2.8$^{a}$ | 34.9 ± 1.5$^{a}$ | <0.001 |
| [2]**tGSH (nmol/mg tissue)** | 3.7 ± 0.2$^{a}$ | 2.8 ± 0.1$^{c}$ | 3.1 ± 0.1$^{bc}$ | 3.3 ± 0.2$^{b}$ | <0.001 |
| [2]**NFκB p65 binding activity (%LF)** | 100 ± 12$^{b}$ | 224 ± 24$^{a}$ | 139 ± 37$^{b}$ | 92 ± 9$^{b}$ | <0.001 |

[1]Data are means ± SE, n = 15–16. Labeled means groups without a common letter differ, $P < 0.05$. GTE, green tea extract; HFD, high-fat diet; HFD+1% GTE, high-fat diet containing 1% green tea extract; HFD+2% GTE, high-fat diet containing 2% green tea extract; LFD, low-fat diet; HOMA-IR, Homeostatic Model Assessment of Insulin Resistance; AST, aspartate aminotransferase; ALT, alanine aminotransferase; tGSH, hepatic total glutathione.
[2]Data previously reported by Park et al [13]
[3]Data in preparation for publication by Chung et al [87]

**Figure 4.2.1** *Histological Evidence of Perisinusoidal Fibrosis* from the liver of rats fed a LFD, HFD, HFD+1% GTE or HFD+ 2% GTE for 8 wk[1]

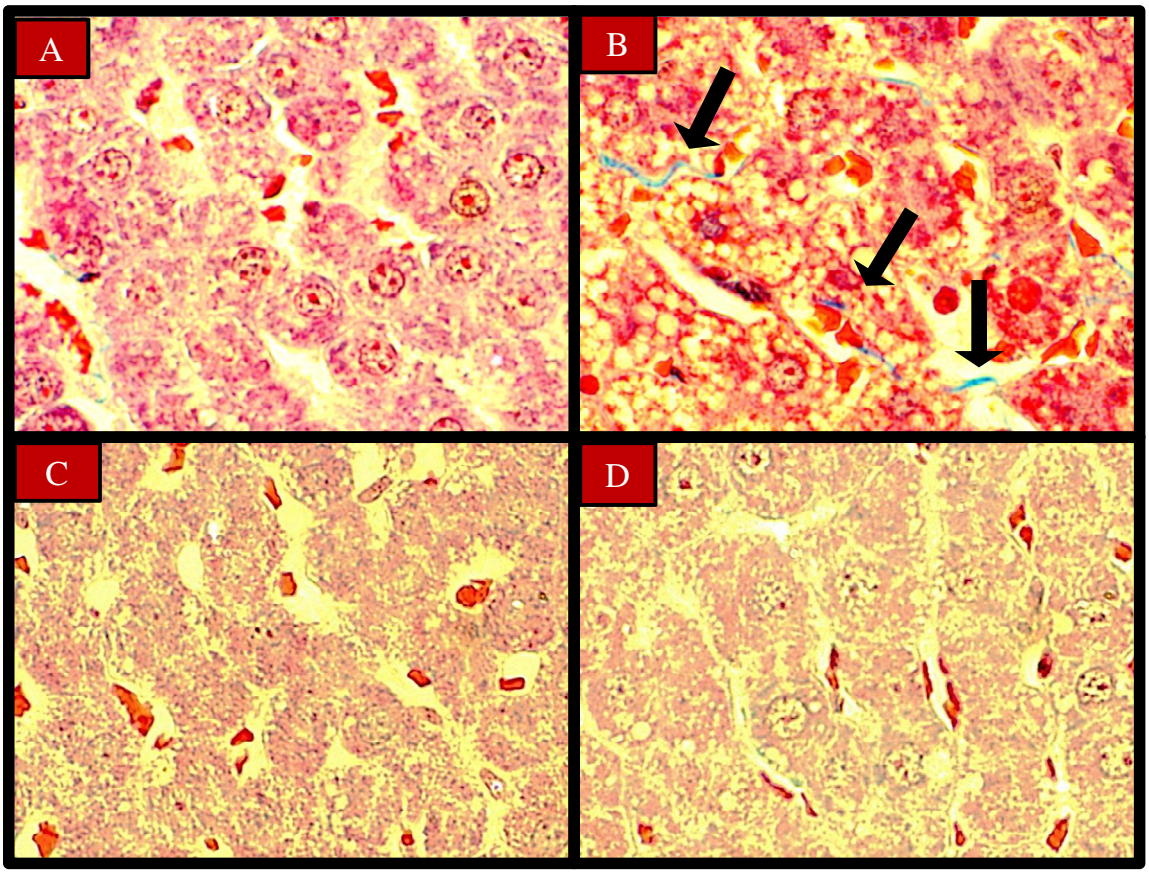


Gomori's trichrome stain, 100×. Arrows indicate the location of collagen deposition. A) Sample liver section from the LFD group. B) Sample liver section from the HFD group. C) Sample liver section from the HFD+1% GTE group. D) Sample liver section from the HFD+2% GTE group.

[1]Abbreviations: GTE, green tea extract; HFD, high-fat diet; HFD+1% GTE, high-fat diet containing 1% green tea extract; HFD+2% GTE, high-fat diet containing 2% green tea extract; LFD, low-fat diet

**Figure 4.2.2** *Concentration of Hepatic Hydroxyproline* measured from the liver of rats fed a LFD, HFD, HFD+1% GTE or HFD+ 2% GTE for 8 wk[1]

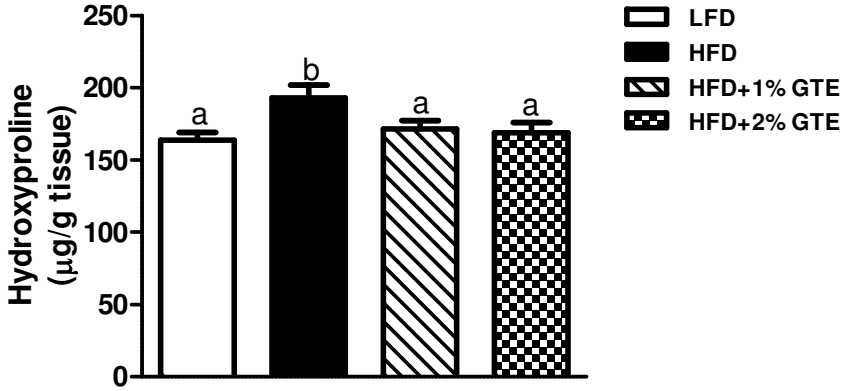


[1]Data are means ± SE, n = 15–16. Labeled means columns without a common letter differ, $P < 0.05$. Abbreviations: GTE, green tea extract; HFD, high-fat diet; HFD+1% GTE, high-fat diet containing 1% green tea extract; HFD+2% GTE, high-fat diet containing 2% green tea extract; LFD, low-fat diet.

**Figure 4.2.3** *Correlations of Liver Injury and Oxidative Stress to Hydroxyproline* measured from rats fed a LFD, HFD, HFD+1% GTE or HFD+ 2% GTE for 8 wk[1]

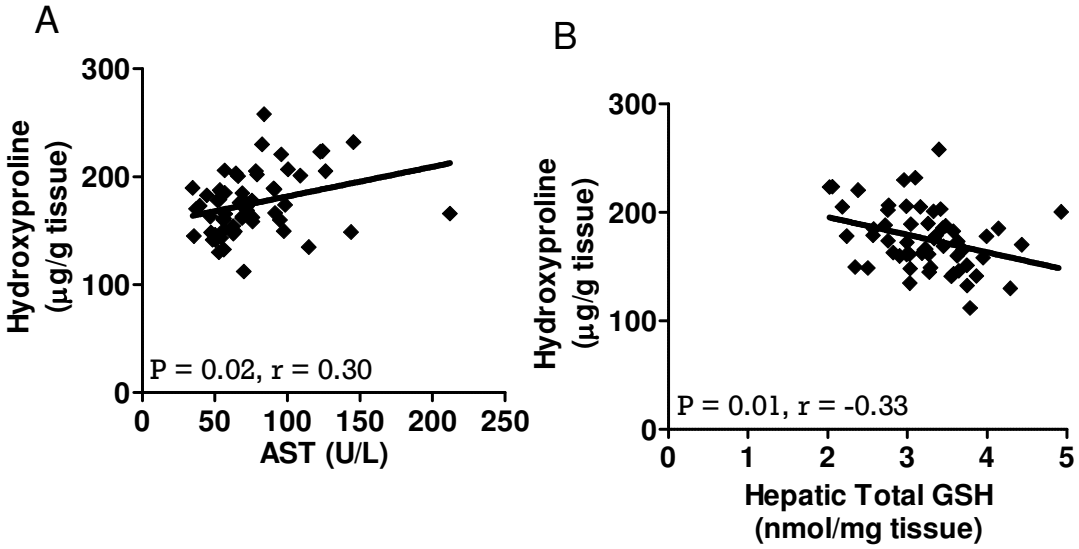


A) There is a significant positive correlation between AST and hydroxyproline concentration. B) There is a significant inverse correlation between tGSH and hydroxyproline concentration.

[1]r represents the Pearson correlation coefficient, P <0.05. Abbreviations: GTE, green tea extract; HFD, high-fat diet; HFD+1% GTE, high-fat diet containing 1% green tea extract; HFD+2% GTE, high-fat diet containing 2% green tea extract; LFD, low-fat diet; α-SMA, alpha-smooth muscle actin; AST, aspartate aminotransferase; tGSH, hepatic total glutathione.

**Figure 4.3.1** *Hepatic α-SMA Protein Expression* measured from the liver of rats fed a LFD, HFD, HFD+1% GTE or HFD+ 2% GTE for 8 wk[1]

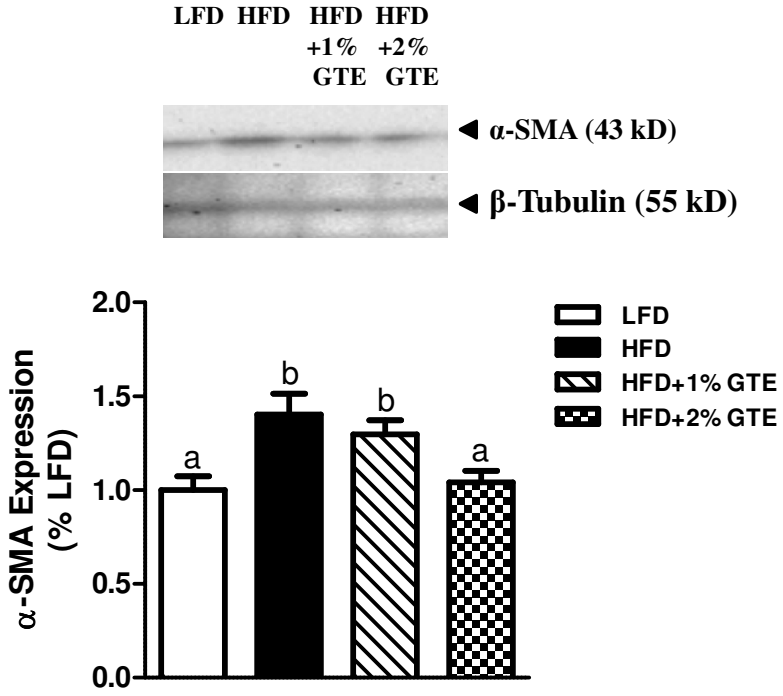


[1]Data are means ± SE, n = 15–16. Labeled means columns without a common letter differ, $P < 0.05$. Abbreviations: GTE, green tea extract; HFD, high-fat diet; HFD+1% GTE, high-fat diet containing 1% green tea extract; HFD+2% GTE, high-fat diet containing 2% green tea extract; LFD, low-fat diet.

**Figure 4.3.2** *Correlations of α-SMA and biomarkers of NASH or fibrosis* measured from rats fed a LFD, HFD, HFD+1% GTE or HFD+ 2% GTE for 8 wk[1]

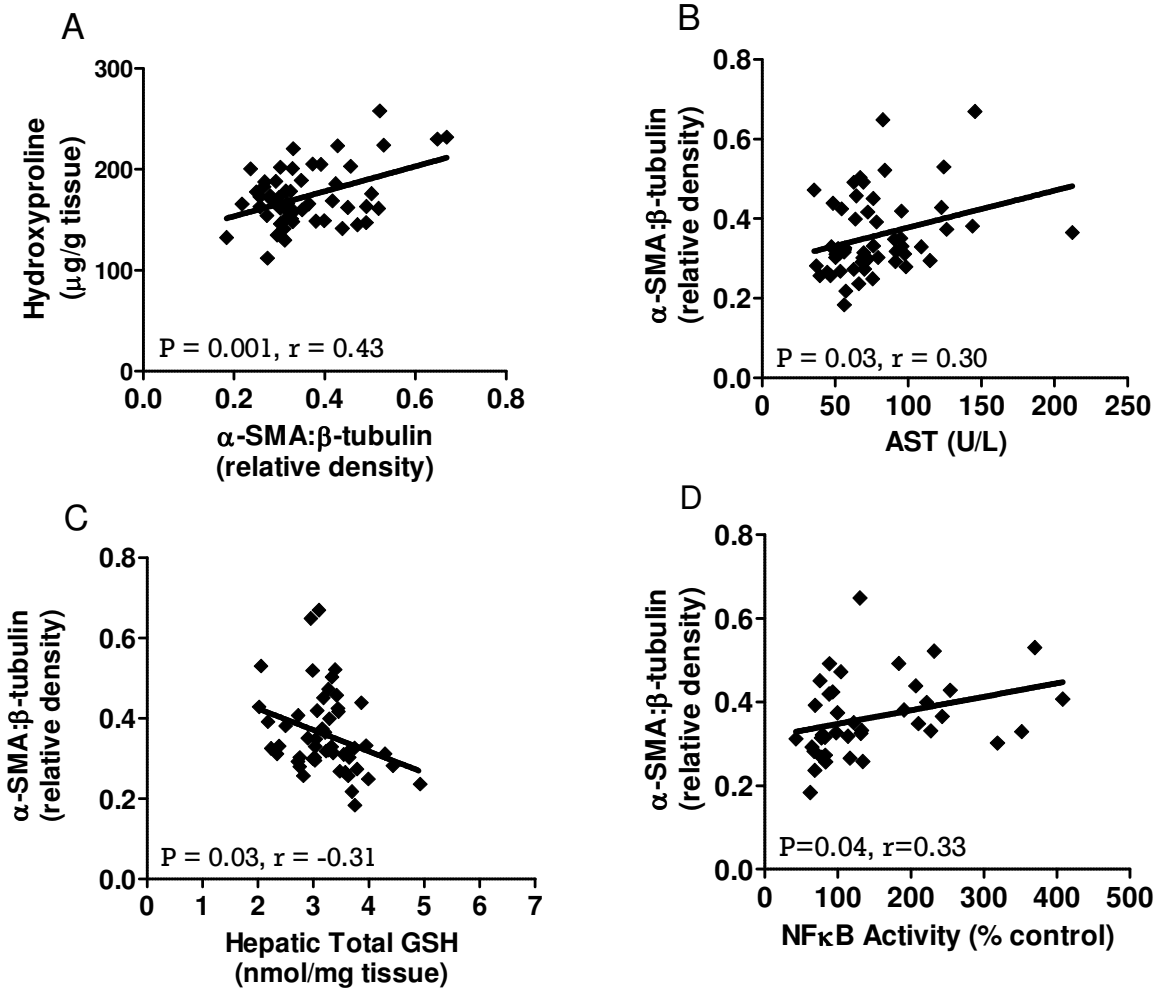


A) There is a significant positive correlation between α-SMA expression and hepatic hydroxyproline concentration. B) There is a significant positive correlation between AST and α-SMA protein expression. C) There is a significant inverse correlation between tGSH and α-SMA protein expression. D) There is a significant positive correlation between NFκB activity and α-SMA protein expression.

[1]r represents the Pearson correlation coefficient, P <0.05. Abbreviations: GTE, green tea extract; HFD, high-fat diet; HFD+1% GTE, high-fat diet containing 1% green tea extract; HFD+2% GTE, high-fat diet containing 2% green tea extract; LFD, low-fat diet; α-SMA, alpha-smooth muscle actin; AST, aspartate aminotransferase; tGSH, hepatic total glutathione; NFκB, nuclear factor kappa-light-chain-enhancer of activated B cells.

**Figure 4.4** *Hepatic Nuclear Protein Expression of KLF6* measured from the liver of rats fed a LFD, HFD, HFD+1% GTE or HFD+ 2% GTE for 8 wk[1]

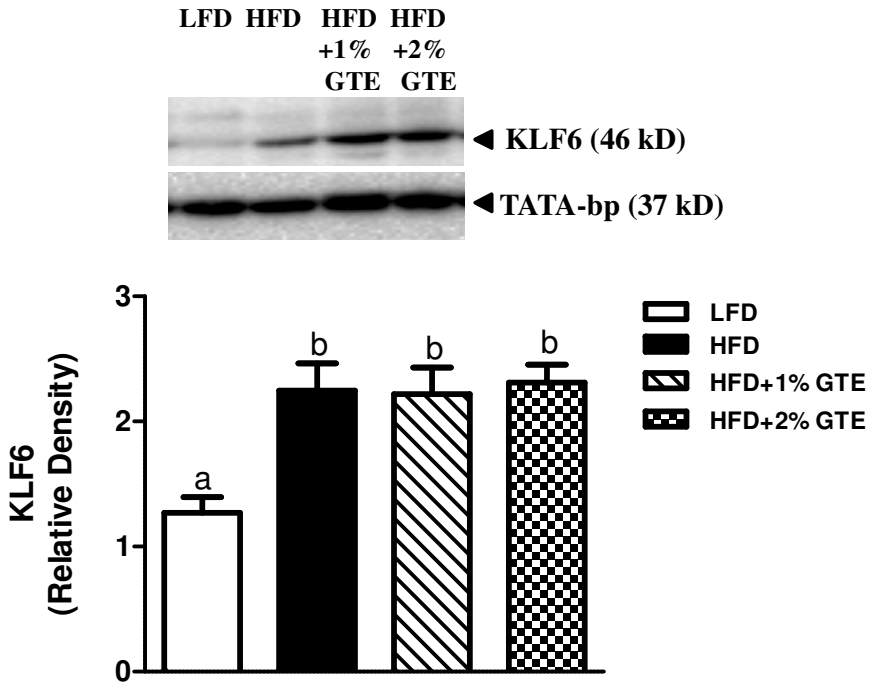


[1]Data are means ± SE, n = 15–16. Labeled means columns without a common letter differ, $P < 0.05$. Abbreviations: GTE, green tea extract; HFD, high-fat diet; HFD+1% GTE, high-fat diet containing 1% green tea extract; HFD+2% GTE, high-fat diet containing 2% green tea extract; LFD, low-fat diet.

# Chapter 5: Discussion

This thesis provides the first evidence in a HFD-induced model of NASH that GTE protects against fibrosis. GTE at 1% and 2%, which is the equivalent to 7 and 14 cups/d of green tea in humans, prevented hepatic fibrosis that was otherwise induced by a HFD as evidenced by a reduction in histologic staining towards collagen and by direct evidence showing that GTE at either level normalized hepatic hydroxyproline concentrations to that of controls fed a LFD. In further support, rats in the HFD + 2% GTE group had less HSC activation as suggested by lower protein expression of α-SMA whereas GTE had no effect on nuclear accumulation of KLF6, which was otherwise increased by a HFD. Collectively, these findings suggest that GTE inhibits the development of fibrosis by suppressing HSC activation, but that the mechanism is independent of the transcriptional effects of KLF6 that are known to promote liver fibrosis [10, 11].

The underlying hypothesis of this thesis, that GTE would protect against fibrosis otherwise induced by a HFD, was based on existing evidence showing that GTE or EGCG protects against chemically-induced [111, 113, 120, 121] or surgically-induced [112, 122] fibrosis. This thesis indicates that consumption of a HFD leads to perisinusoidal fibrosis and that GTE mitigates this effect. This observation was verified by hydroxyproline quantification, since hepatic hydroxyproline concentrations were elevated in the HFD group and were significantly lower in both GTE treatment groups.

Western blot analysis of α-SMA protein expression indicated that the HFD increased HSC activation, while HSC activation was mitigated by GTE at 2% (**Figure 4.3.1**). HSCs are the primary cell types responsible for collagen deposition during fibrosis

[58] and the role of greater HSC activation in fibrosis was supported in thesis by regression analysis that indicated a positive relation between α-SMA and hydroxyproline (**Figure 4.3.2A**). Regression analysis also indicated that there was a positive relation between plasma AST activity and α-SMA expression (**Figure 4.3.2B**) as well as an inverse relation between tGSH and α-SMA expression (**Figure 4.3.2C**). These correlations suggest that greater liver injury and greater oxidative stress are associated with increased HSC activation and are consistent with reports that HSCs are activated by liver injury and oxidative stress [61], since damaged hepatocyte mitochondria release AST [24] and ROS [40] under conditions associated with NAFLD. Several studies in chemically and surgically-induced models of fibrosis, in addition to the model used in this thesis, have reported that GTE or EGCG treatment prevents α-SMA protein expression in addition to preventing collagen deposition in experimental fibrosis [112, 113, 120-122]. Because HSCs are integral in collagen deposition during hepatic fibrosis, GTE may prevent fibrosis by preventing HSC activation.

GTE may mitigate HSC activation and fibrosis by increasing endogenous antioxidant defenses. Increased hepatic GSH was observed in rats fed a HFD containing 1% and 2% GTE for 8 wk [13] and in rats administered ethanol in addition water containing GTE [123] compared to their respective controls. Rats administered ethanol in addition to water containing GTE also had greater hepatic protein levels of Cu/Zn-superoxide dismutase, GSH peroxidase and catalase. These studies indicate that GTE increases antioxidant defenses and that this may protect against fibrosis.

Since antioxidant enzymes scavenge ROS involved in the signaling cascade that leads to increased nuclear binding activity of the redox sensitive transcription factor

NFκB [107] and NFκB promotes the transcription of several genes that initiate and perpetuate fibrosis [63, 64, 114], GTE-mediated increases in antioxidant enzymes may prevent fibrosis. One mechanism by which this may occur is by preventing HSC proliferation. Regression analysis of data regarding hepatic NFκB activity reported previously [13] and data on α-SMA reported in this thesis showed that NFκB activity was positively correlated to α-SMA (**Figure 4.3.2D**). NFκB is responsible for the transcription of PDGF-Rβ [114]. PDGF is expressed by Kupffer cells [69] and promotes HSC proliferation [68]. Since green tea polyphenols reduce hepatic NFκB binding activity [13, 112, 114], it is possible that GTE prevents fibrosis by mitigating HSC proliferation. GTE may also prevent fibrosis by preventing expression of other downstream targets of NFκB that contribute to fibrogenesis. In addition to PDGF-Rβ, NFκB upregulates TNF-α [64] which promotes mitochondrial dysfunction [41] and hepatocyte apoptosis [49] leading to fibrosis. NFκB also upregulates MCP-1 [63], which is a potent chemoattractant for inflammatory cell types and activator of HSCs [1]. Thus, by reducing transcription of these cytokines, GTE may further protect against fibrosis.

GTE-mediated increases in endogenous antioxidant defenses may also prevent fibrosis by interrupting other pro-fibrogenic signaling cascades dependent on ROS. Leptin and TGFβ1 both promote fibrosis by increasing expression of procollagen(α1)I and use $H_2O_2$ as a second messenger upon binding to their receptor [66, 124]. Since GSH peroxidase is responsible for detoxifying intracellular $H_2O_2$ and GTE increases GSH peroxidase activity in animals with NAFLD [104], it is possible that GTE disrupts procollagen(α1)I transcription by increasing hepatic GSH peroxidase. This effect of GTE may also explain why GTE at 1% prevented hepatic collagen accumulation without

affecting HSC activation. While GTE at 1% did not prevent HSC activation, it may have prevented collagen deposition by this cell type by preventing the signaling cascades that lead to procollagen(α1)I transcription by interrupting TGFβ1 and leptin signaling.

GTE-mediated increases in endogenous antioxidant defenses may also protect against fibrosis by preventing the formation of the lipid peroxidation end products 4-HNE and MDA which are hepatotoxic in that they bind to mitochondrial DNA [53], nuclear DNA [54] and proteins [55], which may result in inactivation of important enzymes [27] and lead to fibrosis [1]. 4-HNE and MDA have also been directly implicated in HSC expression of procollagen(α1)I [62, 125]. Previous work in the animals studied in this thesis indicates that hepatic MDA was lower in rats fed a HFD in addition to 1% or 2% GTE compared to the HFD control [87]. Furthermore, rats that underwent bile-duct ligation surgery provided with 50 mg/kg/day of GTE via intragastric administration beginning three days prior to surgery had less immunohistological staining for 4-HNE and α-SMA as well as less histological staining of collagen after 17 days compared to the positive bile-duct ligation control [122]. Thus, these studies indicate that GTE may prevent fibrosis by preventing the harmful effects of lipid peroxidation and formation of its end products.

Another mechanism by which GTE may protect against fibrosis is by preventing hyperleptinemia. Leptin plays an integral role in fibrosis by increasing levels of free TGFβ1 [75], promoting HSC proliferation [77] and by promoting further leptin expression by HSCs [76]. Previous work in this animal model from our lab indicates that consuming 1% or 2% GTE in addition to the HFD decreases circulating leptin [13]. Thus, it is possible that by modulating levels of circulating leptin, GTE prevents fibrosis.

GTE may also protect against fibrosis by preventing obesity and steatosis. Previous work in this model shows that GTE prevents adiposity and steatosis induced by the HFD, independent of energy intake [13]. This may be the result of GTE-mediated elevation in the transcription of the gene for carnitine palmitoyl transferase-1. Carnitine palmitoyl transferase-1 is involved in β-oxidation of free fatty acids [38] and animals fed the HFD+1% GTE and HFD+2% GTE has significantly greater mRNA for this enzyme compared to the LFD and HFD controls [87]. By increasing β-oxidation, GTE may prevent obesity and steatosis independent of energy intake.

KLF6 upregulates procollagen(α1)I transcription as well as transcription TFGβ1 and its receptors [10, 11] and expression of this transcription factor is induced by oxidative stress [83]. Since GTE prevents hepatic fibrosis and mitigates oxidative stress, it was hypothesized that this may be due, in part, to decreased nuclear levels of the transcription factor KLF6. Contrary to the hypothesis, we found that although HFD feeding increased nuclear KLF6, GTE at either dose had no effect on nuclear accumulation of this transcription factor. Because transcriptional upregulation of pro-fibrogenic genes regulated by KLF6 is dependent on cooperation with the transcription factor Sp1 [126], interruption in Sp1 activity may prevent KLF6 from upregulating its target genes. In fact, EGCG has been shown to decrease expression, DNA binding activity and transactivation activity of Sp1 [127, 128]. If Sp1 nuclear activity is inhibited by GTE in HFD-induced fibrosis, then nuclear translocation of KLF6 may still occur, while KLF6 would be unable to promote transcription of its target genes. Thus, future studies should consider examining nuclear translocation of Sp1 in this model as well as to

perform co-immunoprecipitation experiments to determine if KLF6 and Sp1 are interacting in the nuclei of hepatic cells in the GTE treatment groups.

KLF6 contributes to upregulation procollagen(α1) in fibrosis [11] and this thesis reports that GTE prevented hepatic collagen accumulation that was not accompanied by a reduction in KLF6 nuclear accumulation. This necessitates the identification of other contributors to collagen deposition that may have been affected by GTE. Interrupting TGFβ1 and leptin mediating signaling that initiates procollagen(α1)I transcription may be one mechanism by which GTE prevents collagen accumulation independent of KLF6. As previously mentioned, these signaling cascades are depending on $H_2O_2$ [66, 124]. GTE increases endogenous GSH peroxidase [104], which may interrupt this signaling cascade resulting in decreased collagen transcription. Additionally, activated HSCs are the primary cell type responsible for collagen deposition during fibrosis and this thesis has shown that supplementation of GTE at 2% resulted in lower HSC activation. Thus the 2% GTE treatment may have limited collagen deposition by preventing HSC activation, a mechanism independent of KLF6.

A strength of this study is that the HFD-induced NAFLD model replicates certain aspects associated with of fibrosis are not present in other models of fibrosis. The HFD-induced model of fibrosis exhibits hyperleptinemia, hyperlipidemia and insulin resistance [13, 87]. These components are absent in other commonly used model of fibrosis such as CCl4-injection and methionine choline deficiency [129, 130]. As a result of using the HFD model, it is possible to determine the effect of GTE on these parameters in the context of fibrosis and creates a better understanding of the therapeutic potential of GTE.

The difficulty in diagnosing NAFLD [2] suggests that an emphasis should be placed on prevention of this condition over treatment. Thus, another strength of this study is it that it supports further investigation of increased green tea consumption in humans as a therapy to prevent fibrosis. Because of the high prevalence of NAFLD in obese individuals [3] and the rise in obesity over the past two decades [131], identifying a simple therapy that mitigates the progression of NAFLD may protect the health of millions of individuals.

A limitation of this model is that rats fed a HFD to induce NAFLD develop steatosis in a manner different from its pathogenesis in humans. Studies from our lab on this model indicates that animals fed the HFD had significantly lower circulating free fatty acids, total cholesterol and triglycerides, regardless of the green tea treatment. HFD-fed animals also had lower expression of genes involved in *de novo* lipogenesis compared to the LFD which was independent of the GTE treatments [87]. NAFLD in humans is accompanied by increased serum lipids as well as increased *de novo* lipogenesis [27] indicating this model does not perfectly replicate NAFLD in humans. Despite the decreased serum lipids and *de novo* lipogenesis, animals in this study still developed steatosis. This is likely the result of increased hepatic triglyceride synthesis, since animals in the HFD groups had greater gene expression of the enzyme diglyceride acyltransferase-2 [87].

Also, despite consuming the same amount of calories as the LFD group and the green tea treatment groups, animals in the HFD group had significantly greater body weight. As mentioned previously, animals in the green tea treatment groups had greater expression of carnitine palmitoyl transferase-1 which is involved in β-oxidation and this

may account for the difference in body weight. However, animals in the LFD and HFD groups did not have significantly different levels of carnitine palmitoyl transferase-1 and yet the HFD still weighed significantly more than the LFD group. This may be explained in part by the observation that animals in the HFD group has significantly lower blood lipids compared the LFD. This suggests that there is less lipolysis of fatty acids from adipose tissue and less transport of fatty acids out of the liver. This may result in increased accumulation of fat in these sites of lipid storage and thus increase adiposity without a change in energy intake or β-oxidation.

Another limitation of this study is that it cannot distinguish at which stage in the progression of NAFLD that GTE exhibits its anti-fibrogenic effects. It is possible that GTE mitigates fibrosis by mitigating precursor events such as insulin resistance and steatosis. Previous work in this model shows that GTE prevents insulin resistance, hepatic lipid accumulation, transcription of pro-inflammatory cytokines and oxidative stress as indicated by increased hepatic GSH [13, 87], thus GTE may be mitigating NAFLD at any stage. This prevention study should be complimented by treatment studies in order to more fully understanding the therapeutic potential of green tea, since early stages of NAFLD are difficult to diagnose [2].

Lastly, in order to better understand the mechanism by which GTE prevents fibrosis, our protein expression experiments should be complimented by gene expression experiments. Measuring hepatic mRNA levels of α-SMA and procollagen(α1)I would provide insight into how GTE modulates the expression of these proteins. It would also be valuable to measure mRNA levels of TGFβ1 since this cytokine plays an important role in collagen deposition by HSCs [66].

In conclusion, Wistar rats fed a diet containing 60% fat for 8 wk develop obesity, insulin resistance and leptin resistance as well as steatosis and NASH. We have shown for that animals fed this diet over 8 wk also develop fibrosis. Using this model we have also shown that consuming GTE in addition to the HFD mitigates fibrogenesis by reducing HSC activation and thus hepatic collagen deposition and this occurs independent of nuclear KLF6 accumulation. The results of this study are consistent with the findings of others using various other models of fibrosis. Our study is unique in that it indicates that GTE has anti-fibrogenic properties under conditions associated obesity. Furthermore, this study supports investigating increased consumption of green tea in humans as a therapy for preventing the development of fibrosis associated with NAFLD.

# References


1. Bataller R, D. B. Liver fibrosis. Journal of Clinical Investigation 2005; 115:209-218.

2. Vernon G, Baranova A, Younossi ZM. Systematic review: the epidemiology and natural history of non-alcoholic fatty liver disease and non-alcoholic steatohepatitis in adults. Aliment Pharmacol Ther 2011; 34:274-285.

3. Bellentani S, Scaglioni F, Marino M, Bedogni G. Epidemiology of non-alcoholic fatty liver disease. Dig Dis 2010; 28:155-161.

4. Ong JP, Younossi ZM. Epidemiology and natural history of NAFLD and NASH. Clin Liver Dis 2007; 11:1-16, vii.

5. Angulo P. Nonalcoholic Fatty Liver Disease N Engl J Med 2002; 346:1221-1231.

6. Ayyad C, Andersen T. Long-term efficacy of dietary treatment of obesity: a systematic review of studies published between 1931 and 1999. Obes Rev 2000; 1:113-119.

7. Day CP, James OF. Steatohepatitis: a tale of two "hits"? Gastroenterology 1998; 114:842-845.

8. Poli G. Pathogenesis of liver fibrosis: role of oxidative stress. Mol Aspects Med 2000; 21:49-98.

9. Stärkel P, Sempoux C, Leclercq I, Herin M, Deby C, Desager J-P, Horsmans Y. Oxidative stress, KLF6 and transforming growth factor-β up-regulation differentiate non-alcoholic steatohepatitis progressing to fibrosis from uncomplicated steatosis in rats. J Hepatol 2003; 39:538-546.

10. Kim Y, Ratziu V, Choi SG, Lalazar A, Theiss G, Dang Q, Kim SJ, Friedman SL. Transcriptional activation of transforming growth factor beta1 and its receptors by the Kruppel-like factor Zf9/core promoter-binding protein and Sp1. Potential mechanisms for autocrine fibrogenesis in response to injury. J Biol Chem 1998; 273:33750-33758.

11. Ratziu V, Lalazar A, Wong L, Dang Q, Collins C, Shaulian E, Jensen S, Friedman SL. Zf9, a Kruppel-like transcription factor up-regulated in vivo during early hepatic fibrosis. Proc Natl Acad Sci U S A 1998; 95:9500-9505.

12. Babu PV, Sabitha KE, Shyamaladevi CS. Green tea impedes dyslipidemia, lipid peroxidation, protein glycation and ameliorates Ca2+ -ATPase and Na+/K+ -ATPase activity in the heart of streptozotocin-diabetic rats. Chem Biol Interact 2006; 162:157-164.

13. Park HJ, Lee JY, Chung MY, Park YK, Bower AM, Koo SI, Giardina C, Bruno RS. Green tea extract suppresses NFkappaB activation and inflammatory responses in diet-induced obese rats with nonalcoholic steatohepatitis. J Nutr 2012; 142:57-63.

14. Frei B, Higdon JV. Antioxidant activity of tea polyphenols in vivo: evidence from animal studies. J Nutr 2003; 133:3275S-3284S.

15. Kuriyama S, Shimazu T, Ohmori K, Kikuchi N, Nishino Y, Tsubono Y, Tsuji I. Green Tea Consumption and Mortality Due to Cardiovascular Disease, Cancer, and All Causes in Japan. JAMA 2006; 296:1255-1265.

16. Imai K, Nakachi K. Cross sectional study of effects of drinking green tea on cardiovascular and liver diseases. BMJ 1995; 310:693-696.

17. Kiki I, Altunkaynak Z, Altunkaynak M, Vuraler O, Unal D, Kaplan S. Effect of High Fat Diet on the Volume of Liver and Quantitative Feature of Kupffer Cells in the Female Rat: A Stereological and Ultrastructural Study. Obesity Surgery 2007; 17:1381-1388.

18. Xu ZJ, Fan JG, Ding XD, Qiao L, Wang GL. Characterization of high-fat, diet-induced, non-alcoholic steatohepatitis with fibrosis in rats. Dig Dis Sci 2010; 55:931-940.

19. Bugianesi E, Manzini P, D'Antico S, Vanni E, Longo F, Leone N, Massarenti P, Piga A, Marchesini G, Rizzetto M. Relative contribution of iron burden, HFE mutations, and insulin resistance to fibrosis in nonalcoholic fatty liver. Hepatology 2004; 39:179-187.

20. Ratziu V, Giral P, Charlotte F, Bruckert E, Thibault V, Theodorou I, Khalil L, Turpin G, Opolon P, Poynard T. Liver fibrosis in overweight patients. Gastroenterology 2000; 118:1117-1123.

21. Ong JP, Pitts A, Younossi ZM. Increased overall mortality and liver-related mortality in non-alcoholic fatty liver disease. J Hepatol 2008; 49:608-612.

22. Joseph AE, Saverymuttu SH, al-Sam S, Cook MG, Maxwell JD. Comparison of liver histology with ultrasonography in assessing diffuse parenchymal liver disease. Clin Radiol 1991; 43:26-31.

23. Gasbarrini G, Vero V, Miele L, Forgione A, Hernandez AP, Greco AV, Gasbarrini A, Grieco A. Nonalcoholic fatty liver disease: defining a common problem. Eur Rev Med Pharmacol Sci 2005; 9:253-259.

24. Panteghini M. Aspartate aminotransferase isoenzymes. Clin Biochem 1990; 23:311-319.

25. Brunt EM, Janney CG, Di Bisceglie AM, Neuschwander-Tetri BA, Bacon BR. Nonalcoholic steatohepatitis: a proposal for grading and staging the histological lesions. Am J Gastroenterol 1999; 94:2467-2474.

26. Assy N, Minuk GY. Serum aspartate but not alanine aminotransferase levels help to predict the histological features of chronic hepatitis C viral infections in adults. Am J Gastroenterol 2000; 95:1545-1550.

27. Day CP. Pathogenesis of steatohepatitis. Best Pract Res Clin Gastroenterol 2002; 16:663-678.

28. Hotamisligil GS. Inflammation and metabolic disorders. Nature 2006; 444:860-867.

29. Xu H, Barnes G, Yang Q, Tan G, Yang D, Chou C, Sole J, Nichols A, Ross J, Tartaglia L, Chen H. Chronic inflammation in fat plays a crucial role in the development of obesity-related insulin resistance. Journal of Clinical Investigation 2003; 112:1821-1830.

30. Hotamisligil GS, Arner P, Caro JF, Atkinson RL, Spiegelman BM. Increased adipose tissue expression of tumor necrosis factor-alpha in human obesity and insulin resistance. J Clin Invest 1995; 95:2409-2415.

31. Hotamisligil GS, Murray DL, Choy LN, Spiegelman BM. Tumor necrosis factor alpha inhibits signaling from the insulin receptor. Proc Natl Acad Sci U S A 1994; 91:4854-4858.

32. Virkamaki A, Ueki K, Kahn CR. Protein-protein interaction in insulin signaling and the molecular mechanisms of insulin resistance. J Clin Invest 1999; 103:931-943.

33. Shimomura I, Bashmakov Y, Ikemoto S, Horton JD, Brown MS, Goldstein JL. Insulin selectively increases SREBP-1c mRNA in the livers of rats with streptozotocin-induced diabetes. Proc Natl Acad Sci U S A 1999; 96:13656-13661.

34. Shimomura I, Bashmakov Y, Horton JD. Increased levels of nuclear SREBP-1c associated with fatty livers in two mouse models of diabetes mellitus. J Biol Chem 1999; 274:30028-30032.

35. Hotamisligil GS, Budavari A, Murray D, Spiegelman BM. Reduced tyrosine kinase activity of the insulin receptor in obesity-diabetes. Central role of tumor necrosis factor-alpha. J Clin Invest 1994; 94:1543-1549.

36. Brown MS, Goldstein JL. Selective versus total insulin resistance: a pathogenic paradox. Cell Metab 2008; 7:95-96.

37. Li S, Brown MS, Goldstein JL. Bifurcation of insulin signaling pathway in rat liver: mTORC1 required for stimulation of lipogenesis, but not inhibition of gluconeogenesis. Proc Natl Acad Sci U S A 2010; 107:3441-3446.

38. Browning JD. Molecular mediators of hepatic steatosis and liver injury. Journal of Clinical Investigation 2004; 114:147-152.

39. Holm C. Molecular mechanisms regulating hormone-sensitive lipase and lipolysis. Biochem Soc Trans 2003; 31:1120-1124.

40. Yang S, Zhu H, Li Y, Lin H, Gabrielson K, Trush MA, Diehl AM. Mitochondrial adaptations to obesity-related oxidant stress. Arch Biochem Biophys 2000; 378:259-268.

41. Schulze-Osthoff K, Bakker AC, Vanhaesebroeck B, Beyaert R, Jacob WA, Fiers W. Cytotoxic activity of tumor necrosis factor is mediated by early damage of mitochondrial functions. Evidence for the involvement of mitochondrial radical generation. J Biol Chem 1992; 267:5317-5323.

42. Rolo AP, Teodoro JS, Palmeira CM. Role of oxidative stress in the pathogenesis of nonalcoholic steatohepatitis. Free Radic Biol Med 2012; 52:59-69.

43. Zangar RC, Davydov DR, Verma S. Mechanisms that regulate production of reactive oxygen species by cytochrome P450. Toxicol Appl Pharmacol 2004; 199:316-331.

44. Woodcroft KJ, Hafner MS, Novak RF. Insulin signaling in the transcriptional and posttranscriptional regulation of CYP2E1 expression. Hepatology 2002; 35:263-273.

45. Johnston JB, Ouellet H, Podust LM, Ortiz de Montellano PR. Structural control of cytochrome P450-catalyzed omega-hydroxylation. Arch Biochem Biophys 2011; 507:86-94.

46. Keller H, Dreyer C, Medin J, Mahfoudi A, Ozato K, Wahli W. Fatty acids and retinoids control lipid metabolism through activation of peroxisome proliferator-activated receptor-retinoid X receptor heterodimers. Proc Natl Acad Sci U S A 1993; 90:2160-2164.

47. Robertson G, Leclercq I, Farrell GC. Nonalcoholic steatosis and steatohepatitis. II. Cytochrome P-450 enzymes and oxidative stress. Am J Physiol Gastrointest Liver Physiol 2001; 281:G1135-1139.

48. Ribeiro PS, Cortez-Pinto H, Sola S, Castro RE, Ramalho RM, Baptista A, Moura MC, Camilo ME, Rodrigues CM. Hepatocyte apoptosis, expression of death receptors, and activation of NF-kappaB in the liver of nonalcoholic and alcoholic steatohepatitis patients. Am J Gastroenterol 2004; 99:1708-1717.

49. Leist M, Gantner F, Jilg S, Wendel A. Activation of the 55 kDa TNF receptor is necessary and sufficient for TNF-induced liver failure, hepatocyte apoptosis, and nitrite release. J Immunol 1995; 154:1307-1316.

50. Valko M, Leibfritz D, Moncol J, Cronin MT, Mazur M, Telser J. Free radicals and antioxidants in normal physiological functions and human disease. Int J Biochem Cell Biol 2007; 39:44-84.

51. Cheeseman KH. Mechanisms and effects of lipid peroxidation. Mol Aspects Med 1993; 14:191-197.

52. Pryor WA, Porter NA. Suggested mechanisms for the production of 4-hydroxy-2-nonenal from the autoxidation of polyunsaturated fatty acids. Free Radic Biol Med 1990; 8:541-543.

53. Hruszkewycz AM. Evidence for mitochondrial DNA damage by lipid peroxidation. Biochem Biophys Res Commun 1988; 153:191-197.

54. Burcham PC. Genotoxic lipid peroxidation products: their DNA damaging properties and role in formation of endogenous DNA adducts. Mutagenesis 1998; 13:287-305.

55. Houglum K, Filip M, Witztum JL, Chojkier M. Malondialdehyde and 4-hydroxynonenal protein adducts in plasma and liver of rats with iron overload. J Clin Invest 1990; 86:1991-1998.

56. Pan M. Lipid peroxidation and oxidant stress regulate hepatic apolipoprotein B degradation and VLDL production. Journal of Clinical Investigation 2004; 113:1277-1287.

57. Bedossa P, Paradis V. Liver extracellular matrix in health and disease. J Pathol 2003; 200:504-515.

58. Nakatsukasa H, Nagy P, Evarts RP, Hsia CC, Marsden E, Thorgeirsson SS. Cellular distribution of transforming growth factor-beta 1 and procollagen types I, III, and IV transcripts in carbon tetrachloride-induced rat liver fibrosis. J Clin Invest 1990; 85:1833-1843.

59. Martinez-Hernandez A. The hepatic extracellular matrix. I. Electron immunohistochemical studies in normal rat liver. Lab Invest 1984; 51:57-74.

60. Marra F, Pinzani M. Role of hepatic stellate cells in the pathogenesis of portal hypertension. Nefrologia 2002; 22 Suppl 5:34-40.

61. Nieto N, Friedman SL, Cederbaum AI. Stimulation and proliferation of primary rat hepatic stellate cells by cytochrome P450 2E1-derived reactive oxygen species. Hepatology 2002; 35:62-73.

62. Parola M, Pinzani M, Casini A, Albano E, Poli G, Gentilini A, Gentilini P, Dianzani MU. Stimulation of lipid peroxidation or 4-hydroxynonenal treatment increases procollagen alpha 1 (I) gene expression in human liver fat-storing cells. Biochem Biophys Res Commun 1993; 194:1044-1050.

63. Ueda A, Okuda K, Ohno S, Shirai A, Igarashi T, Matsunaga K, Fukushima J, Kawamoto S, Ishigatsubo Y, Okubo T. NF-kappa B and Sp1 regulate transcription of the human monocyte chemoattractant protein-1 gene. J Immunol 1994; 153:2052-2063.

64. Drouet C, Shakhov AN, Jongeneel CV. Enhancers and transcription factors controlling the inducibility of the tumor necrosis factor-alpha promoter in primary macrophages. J Immunol 1991; 147:1694-1700.

65. Knittel T, Muller L, Saile B, Ramadori G. Effect of tumour necrosis factor-a on proliferation, activation and protein synthesis of rat hepatic stellate cells. Hepatology 1997; 27:1067-1080.

66. Garcia-Trevijano ER, Iraburu MJ, Fontana L, Dominguez-Rosales JA, Auster A, Covarrubias-Pinedo A, Rojkind M. Transforming growth factor beta1 induces the expression of alpha1(I) procollagen mRNA by a hydrogen peroxide-C/EBPbeta-dependent mechanism in rat hepatic stellate cells. Hepatology 1999; 29:960-970.

67. Reeves HL, Friedman SL. Activation of hepatic stellate cells--a key issue in liver fibrosis. Front Biosci 2002; 7:d808-826.

68. Pinzani M, Gesualdo L, Sabbah GM, Abboud HE. Effects of platelet-derived growth factor and other polypeptide mitogens on DNA synthesis and growth of cultured rat liver fat-storing cells. J Clin Invest 1989; 84:1786-1793.

69. Friedman SL, Arthur MJ. Activation of cultured rat hepatic lipocytes by Kupffer cell conditioned medium. Direct enhancement of matrix synthesis and stimulation of cell proliferation via induction of platelet-derived growth factor receptors. J Clin Invest 1989; 84:1780-1785.

70. Chen A, Zhang L, Xu J, Tang J. The antioxidant (-)-epigallocatechin-3-gallate inhibits activated hepatic stellate cell growth and suppresses acetaldehyde-induced gene expression. Biochem J 2002; 368:695-704.

71. Friedman SL, Yamasaki G, Wong L. Modulation of transforming growth factor beta receptors of rat lipocytes during the hepatic wound healing response. Enhanced binding and reduced gene expression accompany cellular activation in culture and in vivo. J Biol Chem 1994; 269:10551-10558.

72. Uemura M, Swenson ES, Gaca MD, Giordano FJ, Reiss M, Wells RG. Smad2 and Smad3 play different roles in rat hepatic stellate cell function and alpha-smooth muscle actin organization. Mol Biol Cell 2005; 16:4214-4224.

73. Kilhovd BK, Berg TJ, Birkeland KI, Thorsby P, Hanssen KF. Serum levels of advanced glycation end products are increased in patients with type 2 diabetes and coronary heart disease. Diabetes Care 1999; 22:1543-1548.

74. Lanthier N, Horsmans Y, Leclercq IA. The metabolic syndrome: how it may influence hepatic stellate cell activation and hepatic fibrosis. Curr Opin Clin Nutr Metab Care 2009; 12:404-411.

75. Leclercq I, Farrell G, Schriemer R, Robertson G. Leptin is essential for the hepatic fibrogenic response to chronic liver injury. Journal of Hepatology 2002; 37:206-213.

76. El-Badawy R, Al-Ghamdi A, Al-Mofleh I. Concepts in leptin and liver disease. The Saudi Journal of Gastroenterology 2004; 10:57-66.

77. Lang T, Ikejima K, Yoshikawa M, Enomoto N, Iijima K, Kitamura T, Takei Y, Sato N. Leptin facilitates proliferation of hepatic stellate cells through up-regulation of platelet-derived growth factor receptor. Biochem Biophys Res Commun 2004; 323:1091-1095.

78. Senoo H, Hata R. Extracellular matrix regulates and L-ascorbic acid 2-phosphate further modulates morphology, proliferation, and collagen synthesis of perisinusoidal stellate cells. Biochem Biophys Res Commun 1994; 200:999-1006.

79. Kleinman HK, McGarvey ML, Hassell JR, Star VL, Cannon FB, Laurie GW, Martin GR. Basement membrane complexes with biological activity. Biochemistry 1986; 25:312-318.

80. Davis B. Transforming growth factor beta1 responsiveness is modulated by extracellular collagen matrix during hepatic Ito cell culture. J Cell Physiol 1988; 136:547-553.

81. Dang DT, Pevsner J, Yang VW. The biology of the mammalian Kruppel-like family of transcription factors. Int J Biochem Cell Biol 2000; 32:1103-1121.

82. Kojima S, Hayashi S, Shimokado K, Suzuki Y, Shimada J, Crippa MP, Friedman SL. Transcriptional activation of urokinase by the Kruppel-like factor Zf9/COPEB activates latent TGF-beta1 in vascular endothelial cells. Blood 2000; 95:1309-1316.

83. Cullingford TE, Butler MJ, Marshall AK, Tham el L, Sugden PH, Clerk A. Differential regulation of Kruppel-like factor family transcription factor expression in neonatal rat cardiac myocytes: effects of endothelin-1, oxidative stress and cytokines. Biochim Biophys Acta 2008; 1783:1229-1236.

84. Urtasun R, Cubero FJ, Nieto N. Oxidative Stress Modulates KLF6(Full) and Its Splice Variants. Alcohol Clin Exp Res 2012;

85. Wang Z, Yao T, Pini M, Zhou Z, Fantuzzi G, Song Z. Betaine improved adipose tissue function in mice fed a high-fat diet: a mechanism for hepatoprotective effect of betaine in nonalcoholic fatty liver disease. Am J Physiol Gastrointest Liver Physiol 2010; 298:G634-642.

86. Kirpich IA, Gobejishvili LN, Bon Homme M, Waigel S, Cave M, Arteel G, Barve SS, McClain CJ, Deaciuc IV. Integrated hepatic transcriptome and proteome analysis of mice with high-fat diet-induced nonalcoholic fatty liver disease. J Nutr Biochem 2011; 22:38-45.

87. Chung MY. Green Tea Extract Supresses Cyclooxygenase-2 Mediated Prostaglandin Synthesis in a Rat Model of Dietary Fat Induced Nonalcoholic Steatohepatitis In Preparation;

88. Suliburska J, Bogdanski P, Szulinska M, Stepien M, Pupek-Musialik D, Jablecka A. Effects of Green Tea Supplementation on Elements, Total Antioxidants, Lipids, and Glucose Values in the Serum of Obese Patients. Biol Trace Elem Res 2012;

89. Tokunaga S, White IR, Frost C, Tanaka K, Kono S, Tokudome S, Akamatsu T, Moriyama T, Zakouji H. Green tea consumption and serum lipids and lipoproteins in a population of healthy workers in Japan. Ann Epidemiol 2002; 12:157-165.

90. Iso H, Date C, Wakai K, Fukui M, Tamakoshi A. The relationship between green tea and total caffeine intake and risk for self-reported type 2 diabetes among Japanese adults. Ann Intern Med 2006; 144:554-562.

91. Harbowy ME, Balentine DA, Davies AP, Cai Y. Tea Chemistry. Critical Reviews in Plant Sciences 1997; 16:415-480.

92. Loest HB, Noh SK, Koo SI. Green tea extract inhibits the lymphatic absorption of cholesterol and alpha-tocopherol in ovariectomized rats. J Nutr 2002; 132:1282-1288.

93. Graham HN. Green tea composition, consumption, and polyphenol chemistry. Prev Med 1992; 21:334-350.

94. Lee MJ, Maliakal P, Chen L, Meng X, Bondoc FY, Prabhu S, Lambert G, Mohr S, Yang CS. Pharmacokinetics of tea catechins after ingestion of green tea and (-)-epigallocatechin-3-gallate by humans: formation of different metabolites and individual variability. Cancer Epidemiol Biomarkers Prev 2002; 11:1025-1032.

95. Bruno RS, Dugan CE, Smyth JA, DiNatale DA, Koo SI. Green tea extract protects leptin-deficient, spontaneously obese mice from hepatic steatosis and injury. J Nutr 2008; 138:323-331.

96. Park HJ, DiNatale DA, Chung MY, Park YK, Lee JY, Koo SI, O'Connor M, Manautou JE, Bruno RS. Green tea extract attenuates hepatic steatosis by

decreasing adipose lipogenesis and enhancing hepatic antioxidant defenses in ob/ob mice. J Nutr Biochem 2011; 22:393-400.

97. Shishikura Y, Khokhar S, Murray BS. Effects of tea polyphenols on emulsification of olive oil in a small intestine model system. J Agric Food Chem 2006; 54:1906-1913.

98. Wang S, Noh SK, Koo SI. Green tea catechins inhibit pancreatic phospholipase A(2) and intestinal absorption of lipids in ovariectomized rats. J Nutr Biochem 2006; 17:492-498.

99. Wang S, Noh SK, Koo SI. Epigallocatechin gallate and caffeine differentially inhibit the intestinal absorption of cholesterol and fat in ovariectomized rats. J Nutr 2006; 136:2791-2796.

100. Dulloo AG, Seydoux J, Girardier L, Chantre P, Vandermander J. Green tea and thermogenesis: interactions between catechin-polyphenols, caffeine and sympathetic activity. Int J Obes Relat Metab Disord 2000; 24:252-258.

101. Dulloo AG, Duret C, Rohrer D, Girardier L, Mensi N, Fathi M, Chantre P, Vandermander J. Efficacy of a green tea extract rich in catechin polyphenols and caffeine in increasing 24-h energy expenditure and fat oxidation in humans. Am J Clin Nutr 1999; 70:1040-1045.

102. Yumei F, Zhou Y, Zheng S, Chen A. The antifibrogenic effect of (-)-epigallocatechin gallate results from the induction of de novo synthesis of glutathione in passaged rat hepatic stellate cells. Lab Invest 2006; 86:697-709.

103. Fu Y, Zheng S, Lu SC, Chen A. Epigallocatechin-3-gallate inhibits growth of activated hepatic stellate cells by enhancing the capacity of glutathione synthesis. Mol Pharmacol 2008; 73:1465-1473.

104. Skrzydlewska E, Ostrowska J, Stankiewicz A, Farbiszewski R. Green tea as a potent antioxidant in alcohol intoxication. Addict Biol 2002; 7:307-314.

105. Zhong Z, Froh M, Connor HD, Li X, Conzelmann LO, Mason RP, Lemasters JJ, Thurman RG. Prevention of hepatic ischemia-reperfusion injury by green tea extract. Am J Physiol Gastrointest Liver Physiol 2002; 283:G957-964.

106. Meyer M, Schreck R, Baeuerle PA. H2O2 and antioxidants have opposite effects on activation of NF-kappa B and AP-1 in intact cells: AP-1 as secondary antioxidant-responsive factor. EMBO J 1993; 12:2005-2015.

107. Bowie A, O'Neill LA. Oxidative stress and nuclear factor-kappaB activation: a reassessment of the evidence in the light of recent discoveries. Biochem Pharmacol 2000; 59:13-23.

108. Chung MY, Park HJ, Manautou JE, Koo SI, Bruno RS. Green tea extract protects against nonalcoholic steatohepatitis in ob/ob mice by decreasing oxidative and nitrative stress responses induced by proinflammatory enzymes. J Nutr Biochem 2012; 23:361-367.

109. Leclercq IA, Farrell GC, Sempoux C, dela Pena A, Horsmans Y. Curcumin inhibits NF-kappaB activation and reduces the severity of experimental steatohepatitis in mice. J Hepatol 2004; 41:926-934.

110. Hata AN, Breyer RM. Pharmacology and signaling of prostaglandin receptors: multiple roles in inflammation and immune modulation. Pharmacol Ther 2004; 103:147-166.

111. Abe K, Suzuki T, Ijiri M, Koyama Y, Isemura M, Kinae N. The anti-fibrotic effect of green tea with a high catechin content in the galactosamine-injured rat liver. Biomed Res 2007; 28:43-48.

112. Zhong Z, Froh M, Lehnert M, Schoonhoven R, Yang L, Lind H, Lemasters JJ, Thurman RG. Polyphenols from Camellia sinenesis attenuate experimental cholestasis-induced liver fibrosis in rats. Am J Physiol Gastrointest Liver Physiol 2003; 285:G1004-1013.

113. Yasuda Y, Shimizu M, Sakai H, Iwasa J, Kubota M, Adachi S, Osawa Y, Tsurumi H, Hara Y, Moriwaki H. (-)-Epigallocatechin gallate prevents carbon tetrachloride-induced rat hepatic fibrosis by inhibiting the expression of the PDGFRbeta and IGF-1R. Chem Biol Interact 2009; 182:159-164.

114. Chen A, Zhang L. The antioxidant (-)-epigallocatechin-3-gallate inhibits rat hepatic stellate cell proliferation in vitro by blocking the tyrosine phosphorylation and reducing the gene expression of platelet-derived growth factor-beta receptor. J Biol Chem 2003; 278:23381-23389.

115. Li J, Schmidt AM. Characterization and functional analysis of the promoter of RAGE, the receptor for advanced glycation end products. J Biol Chem 1997; 272:16498-16506.

116. Nobili V, Manco M, Ciampalini P, Diciommo V, Devito R, Piemonte F, Comparcola D, Guidi R, Marcellini M. Leptin, free leptin index, insulin resistance and liver fibrosis in children with non-alcoholic fatty liver disease. Eur J Endocrinol 2006; 155:735-743.

117. Nakachi K, Matsuyama S, Miyake S, Suganuma M, Imai K. Preventive effects of drinking green tea on cancer and cardiovascular disease: epidemiological evidence for multiple targeting prevention. Biofactors 2000; 13:49-54.

118. Reddy KR, Enwemeka C. A Simplified Method for the Analysis of Hydroxyproline in Biological Tissue. Clin Biochem 1996; 26:225-229.

119. Nemethy G, Scheraga HA. Stabilization of collagen fibrils by hydroxyproline. Biochemistry 1986; 25:3184-3188.

120. Zhen MC, Wang Q, Huang XH, Cao LQ, Chen XL, Sun K, Liu YJ, Li W, Zhang LJ. Green tea polyphenol epigallocatechin-3-gallate inhibits oxidative damage and preventive effects on carbon tetrachloride-induced hepatic fibrosis. J Nutr Biochem 2007; 18:795-805.

121. Tipoe GL, Leung TM, Liong EC, Lau TY, Fung ML, Nanji AA. Epigallocatechin-3-gallate (EGCG) reduces liver inflammation, oxidative stress and fibrosis in carbon tetrachloride (CCl4)-induced liver injury in mice. Toxicology 2010; 273:45-52.

122. Kobayashi H, Tanaka Y, Asagiri K, Asakawa T, Tanikawa K, Kage M, Yagi M. The antioxidant effect of green tea catechin ameliorates experimental liver injury. Phytomedicine 2010; 17:197-202.

123. !!! INVALID CITATION !!!;

124. Cao Q, Mak KM, Lieber CS. Leptin enhances alpha1(I) collagen gene expression in LX-2 human hepatic stellate cells through JAK-mediated H2O2-dependent MAPK pathways. J Cell Biochem 2006; 97:188-197.

125. Bedossa P, Houglum K, Trautwein C, Holstege A, Chojkier M. Stimulation of collagen alpha 1(I) gene expression is associated with lipid peroxidation in hepatocellular injury: a link to tissue fibrosis? Hepatology 1994; 19:1262-1271.

126. Botella LM, Sanchez-Elsner T, Sanz-Rodriguez F, Kojima S, Shimada J, Guerrero-Esteo M, Cooreman MP, Ratziu V, Langa C, Vary CP, et al. Transcriptional activation of endoglin and transforming growth factor-beta signaling components by cooperative interaction between Sp1 and KLF6: their potential role in the response to vascular injury. Blood 2002; 100:4001-4010.

127. Ren F, Zhang S, Mitchell SH, Butler R, Young CY. Tea polyphenols down-regulate the expression of the androgen receptor in LNCaP prostate cancer cells. Oncogene 2000; 19:1924-1932.

128. Yeh CW, Chen WJ, Chiang CT, Lin-Shiau SY, Lin JK. Suppression of fatty acid synthase in MCF-7 breast cancer cells by tea and tea polyphenols: a possible mechanism for their hypolipidemic effects. Pharmacogenomics J 2003; 3:267-276.

129. Anstee QM, Goldin RD. Mouse models in non-alcoholic fatty liver disease and steatohepatitis research. Int J Exp Pathol 2006; 87:1-16.

130. Weber LW, Boll M, Stampfl A. Hepatotoxicity and mechanism of action of haloalkanes: carbon tetrachloride as a toxicological model. Crit Rev Toxicol 2003; 33:105-136.

131. World Health Statistics: A Snapshot of Global Health. World Health Organization; 2012.